The United Nations
University

GEOTHERMAL TRAINING PROGRAMME
Orkustofnun, Grensasvegur 9,
IS-108 Reykjavík, Iceland

Reports 1994
Number 10

A REVISED CONCEPTUAL MODEL AND ANALYSIS OF PRODUCTION DATA FOR THE AHUACHAPÁN-CHIPILAPA GEOTHERMAL FIELD IN EL SALVADOR

Julio Eduardo Quijano Cortez
Comisión Ejecutiva Hidroeléctrica del Río Lempa (C.E.L.),
Centro de Investigaciones Geotermicas (C.I.G.),
km 11 ½ Carretera Puerto al Puerto La Libertad,
Santa Tecla, La Libertad,
EL SALVADOR C.A.

ABSTRACT

The Ahuachapán reservoir has been under exploitation for almost 20 years. Temperature and pressure logs from the 32 wells that have been drilled in Ahuachapán and the 8 wells drilled in Chipilapa have been analyzed in order to establish initial formation temperatures and reservoir pressures. The fieldwide distributions of these parameters show that both Ahuachapán and Chipilapa belong to the same geothermal anomaly and suggest an up-flow zone to the south of the present wellfields and a north-northeast trending lateral flow to an outflow area at El Salitre, 7 km north of Ahuachapán. The pressure history of wells in the area shows that the reservoir pressure drawdown caused by fluid production in Ahuachapán is about 17 bars in the production field but extends to the outer part of the geothermal field as far as Chipilapa where the drawdown is of the order 6-7 bars. Ahuachapán and Chipilapa can, therefore, be considered as sub-areas of the same geothermal field. Simple lumped model simulation of the drawdown history shows that the response of Ahuachapán to production during 1975-1985 is that of a liquid-dominated system whereas the pressure history for the last ten years can only be explained by an expanding boiling zone in the reservoir. The reservoir area and permeability estimated from the lumped model are 10-30 km^2 and 30-80 mD, respectively.

1. Introduction

El Salvador is located in Central America at the coast of the Pacific Ocean, south of Honduras. Tectonically, the southern part of Central America is a subduction zone characterized by intensive volcanism. The high-temperature geothermal fields in El Salvador (180-300°C) are associated with this volcanism and seven geothermal fields have been identified (Figure 1).

The Ahuachapán and the Chipilapa geothermal fields are located in the western part of El Salvador. They form a geothermal field about 100 km^2 in areal extent which is associated with the andesitic stratovolcano Laguna Verde. The Ahuachapán geothermal system has been exploited for electrical energy generation since 1975. The geothermal power station is fed by steam from single and double separation of the mass flow from wells. Most of the separated water is disposed to the Pacific Ocean through a 75 km long channel but only a small remaining part is reinjected into the geothermal reservoir. The installed capacity of the power plant is 95 MW_e. It consists of three units, the first and the second (30 MW_e) are fed with high pressure steam only but the third unit (35 MW_e) is fed with both high and low pressure steam. When the operation of the units started (June 1975, June 1976 and November 1980, respectively) rapidly declining reservoir pressures were observed. The pressure drawdown has led to a reduction in the total mass extraction since 1982. The power plant is at present operated within the national grid with the hydropower stations such that geothermal production is lower during the raining season. The annual average production is at present 45 MW_e. The Chipilapa geothermal area has been intensively explored for the last 5 years and seven wells have been drilled ranging from 1500 to 2600 m in depth.

In the following work, an analysis is made on the initial pressure and temperature distribution in the two fields. This is followed by some observations on the changes that can be seen in the temperature and the pressure history of the two fields. On the basis of this a revised conceptual reservoir model covering both Ahuachapán and Chipilapa is presented. Finally, the production history is simulated by using a lumped parameter model and the future performance of the field predicted.

2. A general outline for the Ahuachapán and Chipilapa geothermal fields

The first studies of geothermal resources in the Ahuachapán-Chipilapa geothermal area were carried out in the period 1965-1971 by the Executive Hydroelectric Commission of the Lempa River (CEL) with the participation and advice of the United Nations Development Programme (UNDP). Under this programme 10 deep wells were drilled, identifying a 220-240°C geothermal reservoir (Romagnoli et al., 1976). The deep drilling continued and by the year 1981 a total of 32 wells were completed, ranging from 590 to 1520 m

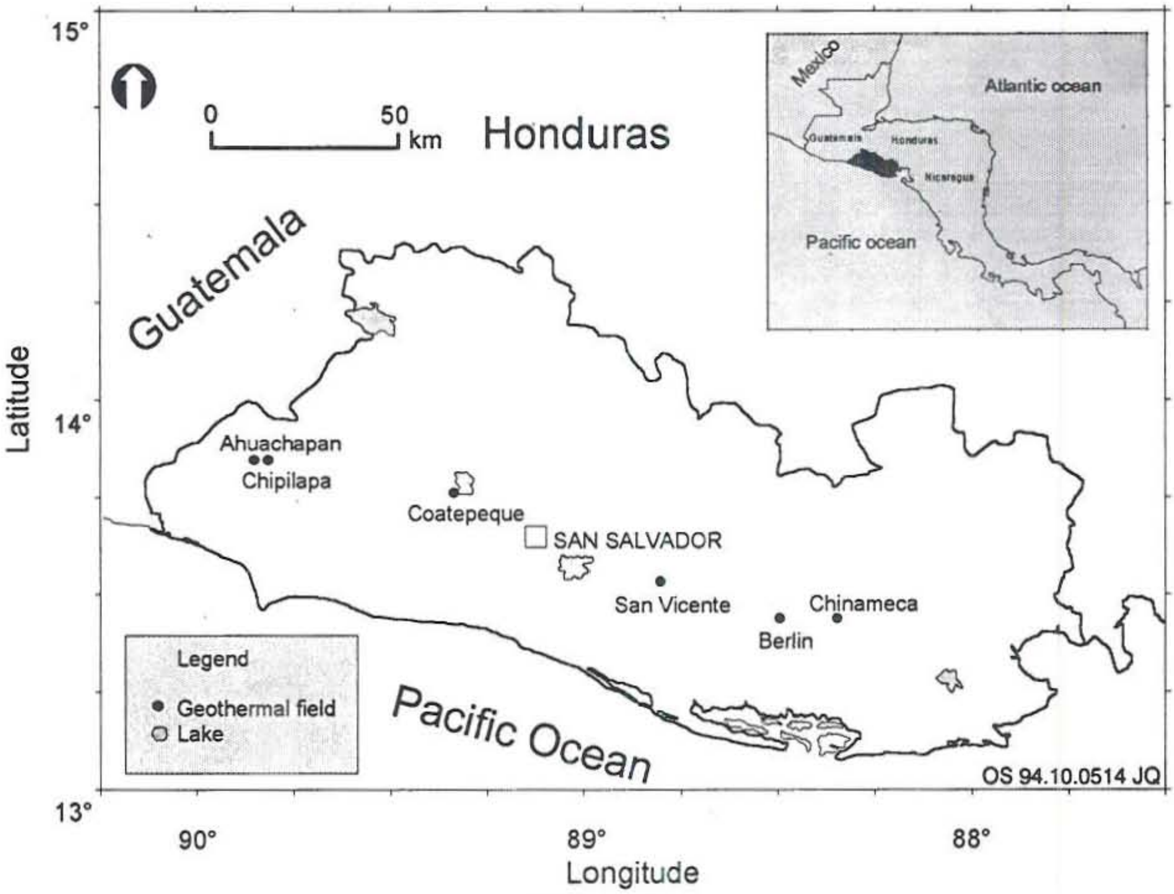

FIGURE 1: Location of high-temperature geothermal fields in El Salvador

depth. Of these wells, 17 have been used as production wells and 5 as reinjection wells, with the remainder non-productive and only used for monitoring. Up to present about 620×10^6 tons of fluid have been extracted from the Ahuachapán reservoir. Figure 2 shows the locations of the wells and Table 1 gives an overview of the production characteristics of the Ahuachapán and Chipilapa wells drilled to date. General information about the wells is also presented in Appendix I.

TABLE 1: Flow characteristics of productive wells in Ahuachapán and Chipilapa (1992-1993)

Well no.	WHP (bar-a)	Total flow (kg/s)	Steam quality (%)	Enthalpy (kJ/kg)
AH-1	6.1	55.2	10	890
AH-6	6	15.8	78	2397
AH-7	6.1	39.6	13	958
AH-17	6.5	15.2	100	2770
AH-19	9.1	46.8	14	955
AH-20	7.2	61.3	20	1094
AH-21	7.8	86.1	15	988
AH-22	6.1	18	34	1404
AH-23	6.1	35.4	22	1289
AH-24	6.3	35.7	15	1003
AH-26	5.8	19.4	43	1595
AH-27	6	58.2	25	1278
AH-28	6	58.1	13	950
AH-31	6.4	79.1	14	962
AH-32	6.5	71.4	14	998
CH7bis	3	19	21	965
CH-9	4.7	46	11	850
CH-D	5.5	19	26	975

Two deep and non-productive wells were drilled in the Chipilapa geothermal field during 1965-1971 (CH-1 and CHe-1). The drilling was reactivated in the period 1989-1993, when seven deep wells ranging from 1500 to 2600 m were completed (Figure 2). In general, the exploration results show that the wells CH-7, CH-8 and CH-A intersect low permeable zones and are non-productive. Only wells CH-7bis, CH-9 and CH-D, adjacent to the eastern boundaries of the Ahuachapán field intersect a permeable zone of temperature at 180-220°C. The permeable zone is composed of andesitic rocks, probably associated with the main production reservoir of Ahuachapán (CFG, 1992). However, the feedzone temperatures are low, resulting in low wellhead pressures during flow. Therefore, the area is at present considered as a possible injection field, for the separated fluid produced in Ahuachapán.

2.1 Reinjection into the Ahuachapán reservoir

Disposal of geothermal waste water has been of major concern in the development of the Ahuachapán field. The first experiments were conducted in 1971, when 150°C fluid from wells AH-1 and AH-6 was injected into well AH-5 for a period of one year. This experiment showed that reinjection was a feasible solution to the disposal problem (Einarsson et al., 1976). As exploitation began, a large scale reinjection project was

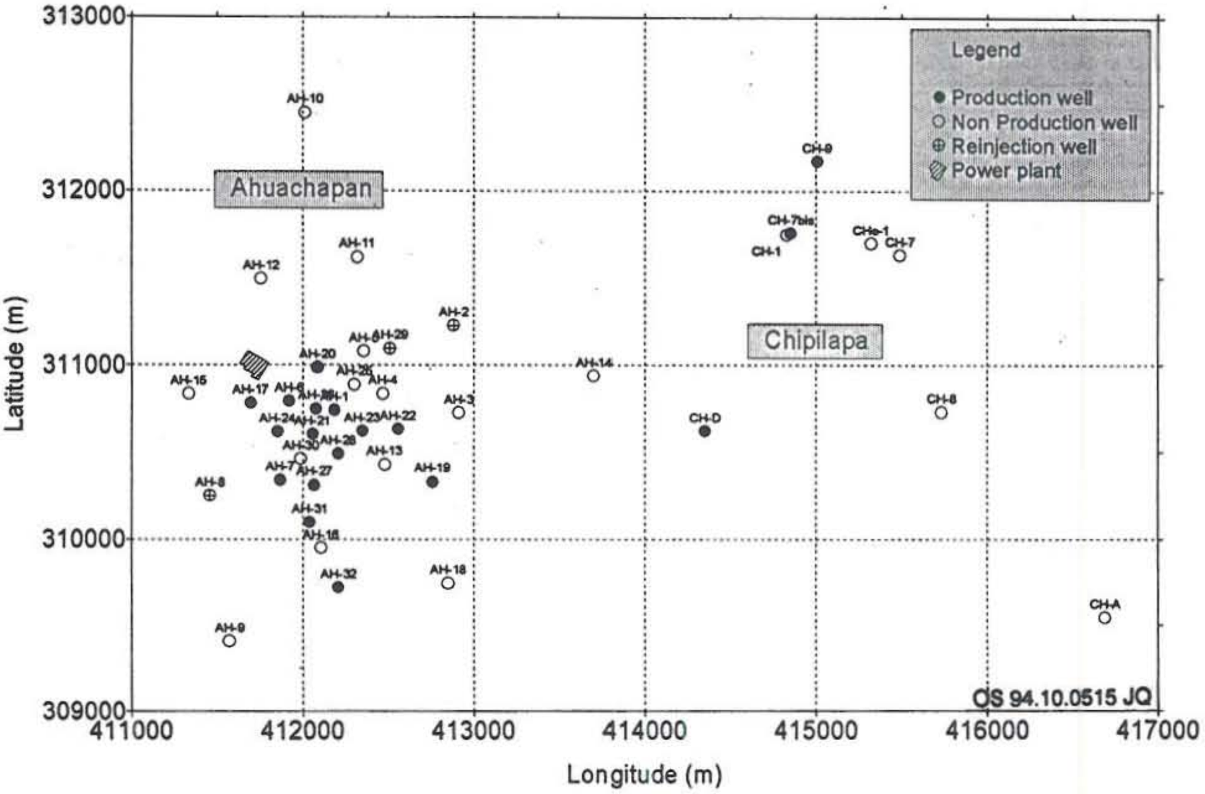

FIGURE 2: Location of wells in the Ahuachapán and Chipilapa geothermal fields

carried out during 1975-1982 using wells AH-2, AH-8, AH-17, AH-19 and AH-29 as injectors (Figure 2). In 1975 as much as 50% of the produced fluid was reinjected, but on the average about 25-30% of the produced fluid injected back to the reservoir at 150°C during the injection years. The reinjection was stopped in October 1982, except for AH-2 where reinjection was continued. Since then most of the waste water is passed to the Pacific Ocean using a 75 km long concrete channel.

TABLE 2: An overview of reinjection wells used during the period 1975-1982

Well no.	Injection period	Water injected (Mtons)
AH-2	Mar. 76-Mar. 93	13.3
AH-8	Jun. 76-May 82	7.3
AH-17	Oct. 76-Jun. 78	5.4
AH-29	May 76-Oct. 82	12
AH-19	Jul. 80-Mar. 81	0.5
Total		38.5

During the reinjection period, the injection into the wells AH-17 and AH-19 was stopped due to a continuous rise in their wellhead pressures. Therefore, the operation of these wells shifted from reinjection to production (Table 2). At the end of the reinjection period in 1982, a total of about 36×10^6 tons of separated water had been reinjected. Most of this water (23×10^6 tons) was reinjected into wells AH-29 and AH-2. This led to a cooling of the reservoir in the vicinity of well AH-29 and lowering of temperatures in well AH-5 and AH-25

(LBL, 1989). The reinjection is also believed to be responsible for a pronounced cooling of about 15-20°C around well AH-8. Also observed, was a rise in the wellhead pressure of wells AH-8 and AH-29. At present only well AH-2 is used as an injector for the separated water from well AH-1.

2.2 Geology of Ahuachapán

Stratigraphically, El Salvador is almost entirely made of Tertiary to Holocene volcanic rocks and debris. These have been classified into basaltic, intermediate and acidic rocks (Wieseman, 1975). The formations identified are:

San Salvador (Pleistocene?-Holocene)
Cuscatlan (Pliocene-Pleistocene)
Balsamo (Miocene?-Pliocene)
Chalatenango (Miocene?)
Morazan (Oligocene)
Metapan (Jurassic?-Cretaceous-Tertiary)

The Ahuachapán geothermal field is located in the northern sector of the Laguna Verde volcanic group on the southern flank of the central Salvadorean graben (Figure 3). Lithologically, the Ahuachapán reservoir lies mostly within the San Salvador formation with only the basement rocks from Balsamo. On the basis of the lithological logs from wells, four major units have been defined (Aumento et al., 1982). They are, surface materials, young agglomerates, Ahuachapán andesites, and older agglomerates. Table 3 gives information on these formations in the Ahuachapán area.

The surface materials in the uppermost 100-150 m, are composed of a series of pyroclastics and lavas. These are associated with groundwater zone, the so-called "Shallow aquifer" (Romagnoli et al., 1976; Cuéllar et

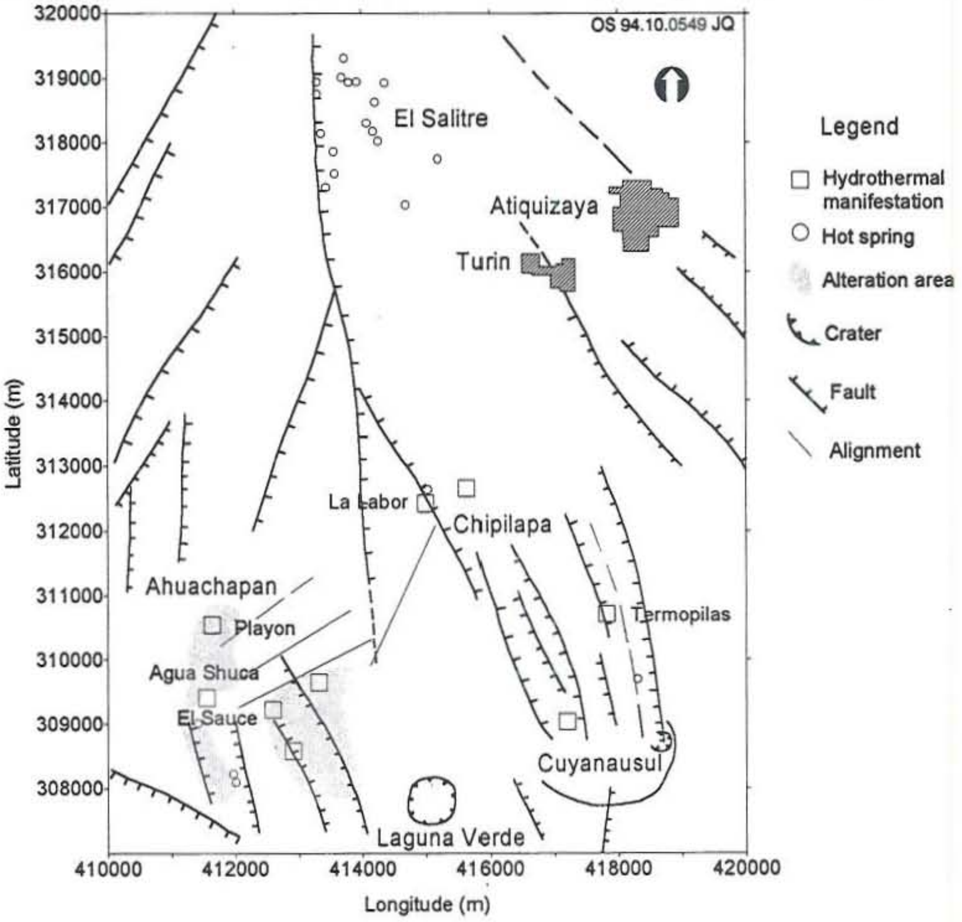

FIGURE 3: Hydrothermal manifestations and the main fault systems of the Ahuachapán-Chipilapa area

al., 1981). Beneath this unit, reside the young agglomerates, a sequence of pyroclastics and andesites ranging in thickness from 300 to 800 m. Circulation losses in these units are attributed to the so-called "Regional saturated aquifer".

TABLE 3: Geological description of the Ahuachapán formations (data from LBL, 1989)

Formation	**Rock type**	**Designation**	**Aquifer**	**Temperature (°C)**	**Salinity (ppm)**
San Salvador (Quaternary)	Colluvium, altered pyroclastics and lavas (Holocene)	Surface materials	Shallow aquifer	40-100	500
	Pyroclastics, andesites (Pleistocene)	Young agglomerates	Regional saturated aquifer	110-130	400
	Andesites (Plio-Pleistocene)	Ahuachapán andesites	Saline aquifer	180-240	22000
Bálsamo (Pliocene)	Breccias, andesites	Older agglomerates	Saline aquifer	180-240	22000

Below the young agglomerates are the Ahuachapán andesites, a highly fractured andesite unit that presents the most permeable reservoir zone. Secondary permeability in this unit is related to columnar jointing and to contact surfaces between different layers. The thickness of the Ahuachapán andesites unit ranges from 200 to 600 m. The older agglomerates are a combination of dense breccias and andesites with low matrix permeability, but contain some fractures (LBL., 1989).

2.3 An outline of the Chipilapa geology

Two types of volcanism can be identified in the Chipilapa area, Plio-Pleistocene and Quaternary volcanism (IIE, 1992). Geochemical data were used to define the different volcanic units observed on the surface. The main stratigraphical units in the Chipilapa area are the following:

1) Plio-Pleistocene rocks. The local basement is characterized by a sequence of agglomerates of lava fragments embedded in ash matrix, lava flows with intermediate-basaltic breccias and scorias. Petrographically these rocks are andesitic lavas with a holocrystaline texture with microlithic matrix and phenocryst of labradorite and pyroxene. This unit is found in the southern part of the Chipilapa area.

2) Quaternary rocks. According to the regional studies of surface geology of the Ahuachapán and the Chipilapa areas, the main lithological units exposed are andesitic-dacitic domes, basaltic-andesitic lava and pumitic pyroclastic.

2.4 Geochemistry

A general model of the hydrothermal system has been developed, which gives the estimated subsurface temperatures and the genetic origin of the fluids with respect to the other types of waters from the subsurface. This includes the chemical analysis of water samples from hot springs and wells, isotopic analysis of the natural water and volatile components of the fumaroles. The model states that a flow of hot water to the surface exists through faults mostly trending NW-SE. The fumaroles at Las Termopilas and El Playon are fed by these faults, which by gas geothermometers give temperatures greater than 200°C (Figure 3). The hydrothermal manifestations of Agua Shuca, El Sauce, La Labor and Chipilapa are fed by steam at lower temperature conditions, 140-180°C (Nieva et al., 1990).

A marked increase in hydrogen content of fumarole steam toward the volcanoes southeast of the Ahuachapán area, suggest that an up-flow zone is probably located beneath the Laguna Verde volcanic complex. The temperature of this upwelling fluid is believed to be 250°C or higher, as suggested by geochemical temperature of the discharged fluid (Laky et al., 1989). Only a small branch of this up-flow feeds the Chipilapa area, possibly through the Escalante fault, where it mixes with shallow waters. These mixed fluids could emerge very diluted through the hydrothermal manifestations of La Labor and Chipilapa.

Most of the up-flowing fluids from Ahuachapán flow to the north. The main outflow for this system is the El Salitre area, located about 7 km north of the Ahuachapán field where more than 1000 l/s of 68-70°C water were discharged prior to the exploitation in Ahuachapán. The fluid of El Salitre was a mixture of geothermal water (10-20%) and shallow aquifer fluid (Glover, 1970). The mixing is believed to occur in the vicinity of the springs. Domestic wells and cold springs to the northeast (Turín-Atiquizaya) are characterized by chloride content of 150-350 mg/l (Figure 3). This may indicate a probable mixture of the sodium-chloride rich geothermal fluid (probably derived from Ahuachapán-Chipilapa) and ground water with low salinity. A maximum reservoir temperature of 250-270°C (Na-K geothermometer) has been estimated for the hot springs and fumaroles shown in Figure 3.

2. TEMPERATURE DISTRIBUTION IN THE AHUACHAPÁN-CHIPILAPA AREA

2.1 Estimation of formation temperatures in wells

In this chapter a brief description is given on the formation temperature and pressure evaluation that was carried out for the Ahuachapán-Chipilapa wells. The formation temperature can be estimated during drilling by measuring the temperature recovery for several hours at the present wellbottom. Several empirical and analytical methods are then applied for estimating the final temperature that would be obtained on full recovery, given that only conductive heat transfer takes place. The most popular methods available to estimate the formation temperature from the temperature recovery data, are the Horner plot method and the Albright method (Helgason, 1993).

In cases where no temperature recovery is measured the only way to estimate the formation temperature is from analysing static profiles in the wells. For the Ahuachapán wells, the data available for this study are the measurements of temperature and pressure collected during the warm-up period of the wells and the static monitoring surveys of pressure and temperature, that are carried out twice every year in most of the wells. The first thing checked in the profiles were two-phase conditions as most of the wells have a boiling zone at shallow depth. The boiling zone identification consisted of comparing old pressure and temperature profiles with the boiling curve with depth. By doing this, a match point was defined between the boiling curve and the measured profiles. Above this match point, boiling curve with depth conditions were assumed, whereas maximum observed temperatures were used to define the formation temperature below the match point. Similarly, the reservoir pressure was defined according to the boiling curve with depth. Below the match point however, the formation temperature was used to define the water density and consequently, the reservoir pressure was determined by using the programme PREDYP (Arason and Bjornsson, 1993). Figure 4 shows an example of the formation temperature evaluation for well AH-1.

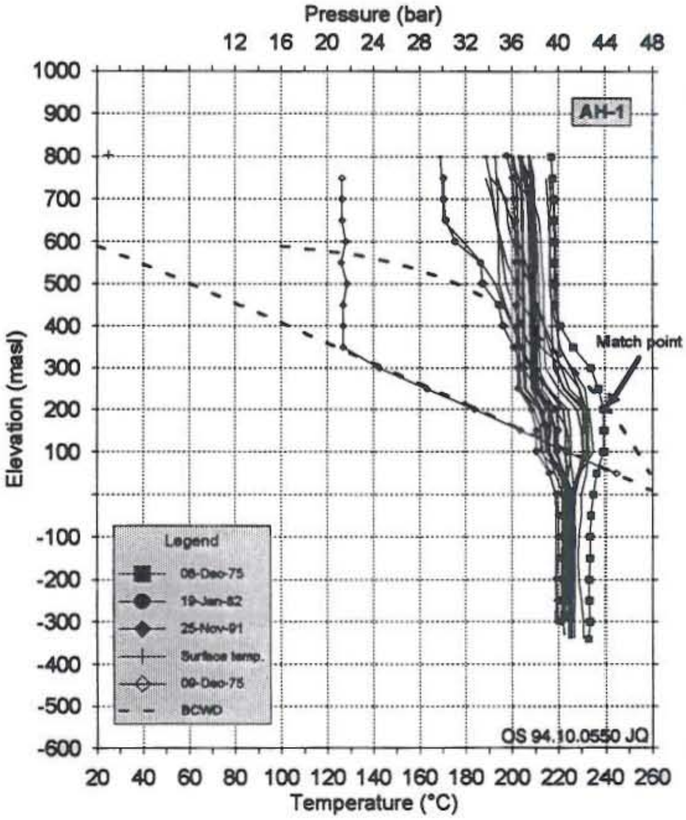

FIGURE 4: Temperature profiles collected in well AH-1, by placing the boiling curve with depth on top of measured data a match point is defined; the reservoir is assumed to be boiling above the match point and in single-phase below it

Wells drilled after 1975 needed a special treatment. During 1975-1985 an average pressure drawdown of 1.3 bar/year took place. This drawdown required an upward shift of the first pressure profile collected in order to establish the reservoir pressure in 1975. The shifted pressure profile along with the measured temperatures was then used to define the match point. For wells with only liquid-phase conditions, the formation temperature is generally based on either the oldest temperature profile or the maximum observed temperature. The estimated formation temperature profiles for all the wells are shown in Appendix II.

2.2 Temperature distribution in the Ahuachapán-Chipilapa area

When the formation temperature profile for each well was at hand several temperature maps and cross-section were drawn for the Ahuachapán-Chipilapa area. Figure 5 presents examples of the temperature distribution at 200 m a.s.l. and at sea level. Also shown is a cross-section from west to east through the area. At shallow depth (200 m a.s.l.) the most dominant feature is a 220°C temperature anomaly in the Ahuachapán wellfield with a mild trend towards Chipilapa. At greater depth (sea level) however, this anomaly has vanished and a new one of temperature higher than 230°C shows up. This anomaly originates at the slopes of the Laguna Verde volcano and strikes north-northeast towards the El Salitre hot springs. This can be interpreted as a recharge into the southern part of the area which then flows laterally to the north-northeast. Furthermore, the cross-section shows reversed temperatures in the depth interval of the Ahuachapán andesites and reflects their high lateral permeability. This suggests that both fields are fed by the single north-northeast trending temperature anomaly shown in Figure 5b. Another feature of interest in the cross-section in Figure 5c is the very "cold" formation temperature near wells CH-8 and CH-A at -200 to -1100 m a.s.l. This reversal is most easily explained by colder recharge from the east.

3. ANALYSIS OF TEMPERATURE AND PRESSURE CHANGES WITH TIME

The near 20 year exploitation of the Ahuachapán field has had a significant effect on the reservoir. During 1975-1986 a gradual decline in reservoir pressure of ~10 bars and temperature of 10-15°C was measured within the main production zone. Temperature changes were also observed deep in the reservoir in a few wells and on the periphery of the wellfield (LBL, 1989). The temperature changes are mainly results of the pressure drawdown. However, the reinjection seems to have caused decline in temperatures of some production wells located near the reinjectors. Figure 6 shows an example of measured pressures and temperatures in wells AH-13 and AH-18 together with the saturation line.

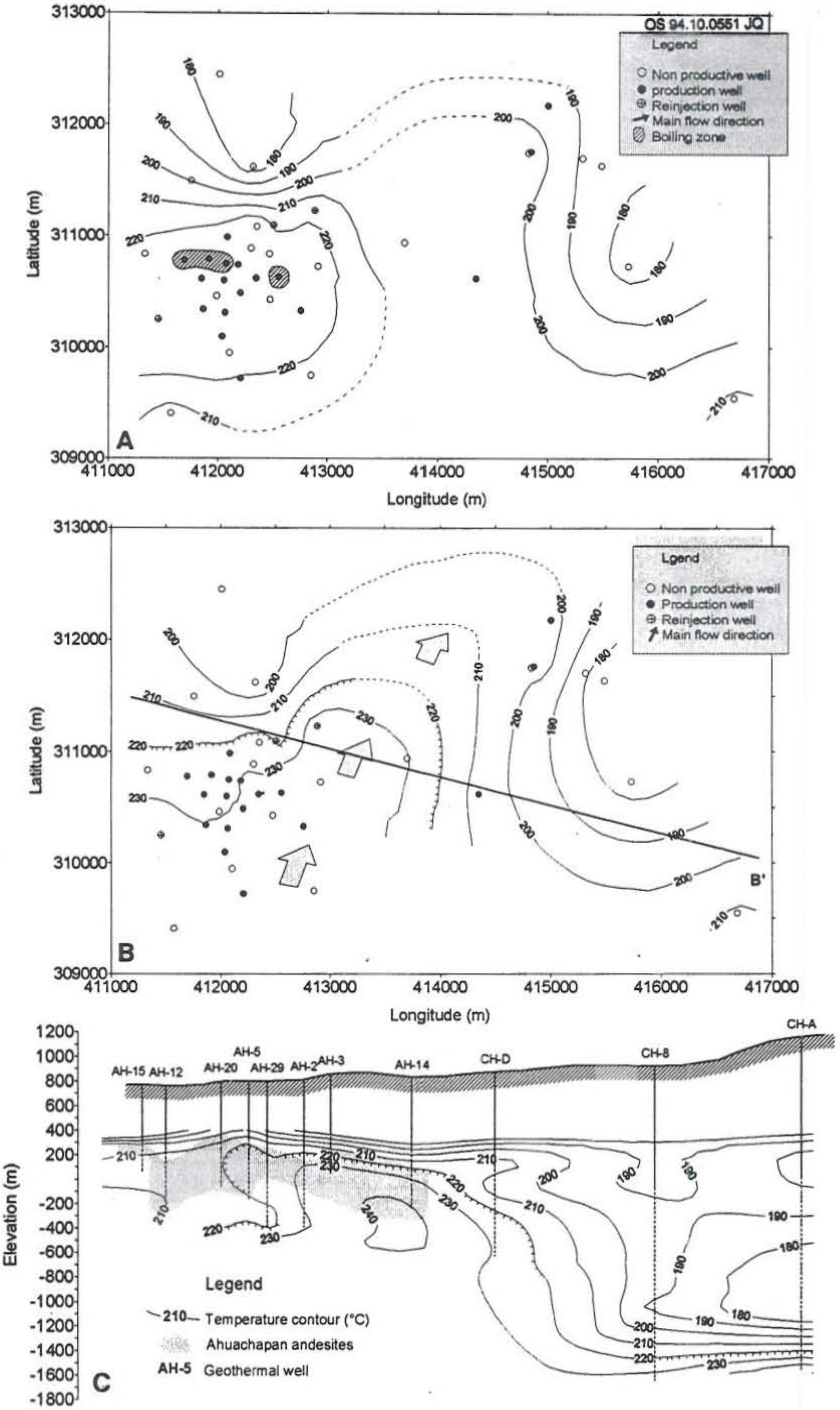

FIGURE 5: Formation temperatures in Ahuachapán-Chipilapa field, a) the distribution at 200 m a.s.l., b) the distribution at sea level, c) a W-E trending cross-section through the field

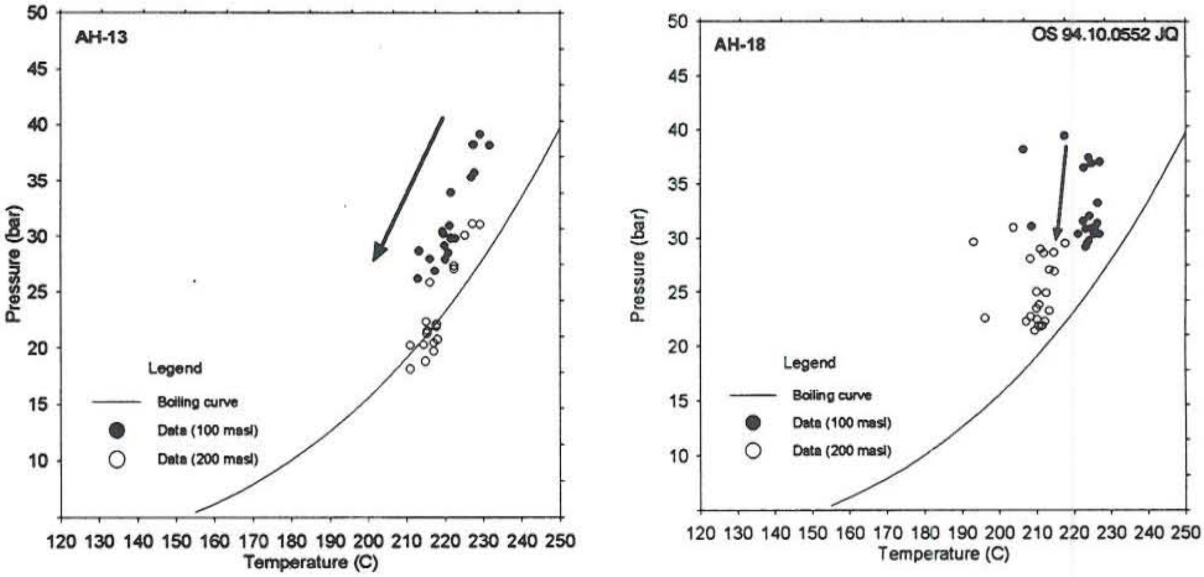

FIGURE 6: Downhole pressure as a function of temperature for the wells AH-13 and AH-18; the data shown are collected during the period 1975-1993, arrows indicate the direction of time

The two-phase region in well AH-13 (200 m a.s.l.) shows cooling along the saturation line. Figure 6 also shows that liquid-dominated reservoir is cooled parallel to the saturation line (AH-13 at 100 m a.s.l. and AH-18). This unusual behaviour is explained by a two-phase recharge with temperatures controlled by the pressure drawdown (LBL, 1989).

The pressure data from the Ahuachapán and Chipilapa wells have been analysed with possible hydrological connection between the two fields in mind. In order to show this, the pressure history of several wells from the fields is shown in Figure 7 at a reference depth of 200 m a.s.l. The initial reservoir pressure in Ahuachapán at this depth was 36 bars whereas the pressure in Chipilapa was initially about 33 bars, according to the pressure logs in well CH-1 in 1969. The pressure in Figure 7 shows that the wells in the Ahuachapán production area have experienced a pressure draw-down of about 17 bars during the last 20 years, well AH-14 which is located half way between Ahuachapán and Chipilapa shows a drawdown of 8 bars, and finally the wells in Chipilapa show 6-7 bars lower pressure today than measured in 1969. Unfortunately, it has not been possible to monitor the pressure in well CH-1 because of an obstruction at a shallow depth, but well CH-7bis which was drilled in 1991 is located only 30 m from CH-1. The present pressure in this well at 200 m a.s.l is 26 bars.

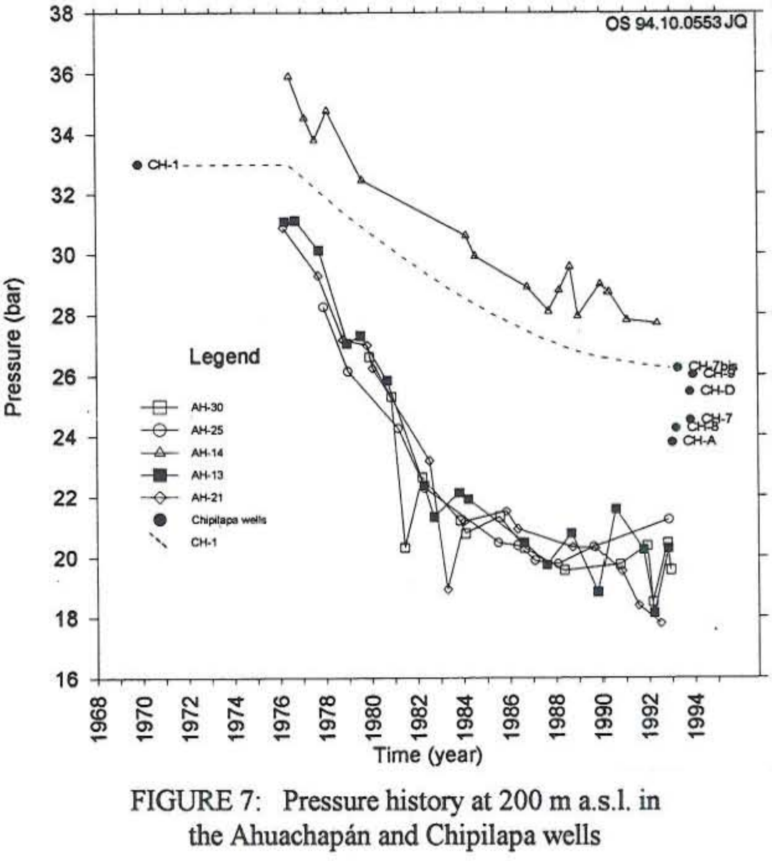

FIGURE 7: Pressure history at 200 m a.s.l. in the Ahuachapán and Chipilapa wells

That means that the Chipilapa reservoir has experienced a pressure drop of about 7 bars as a result of the exploitation of the Ahuachapán reservoir. The data in Figure 7, therefore, show that the Ahuachapán and the Chipilapa reservoirs are hydrologically connected.

It is of interest to note that the Chipilapa area was initially downstream from the Ahuachapán reservoir (in terms of pressure). At present, however, the Chipilapa wells show 4-7 bars higher pressure than in Ahuachapán. The pressure interference between these areas and the lateral gradient show that fluid reinjected in Chipilapa should eventually show up in the Ahuachapán field, but possibly also in the El Salitre hot springs. Another thing of interest is that the initial reservoir pressure in Ahuachapán and Chipilapa was lower than the pressure in a hydrostatic column extending from the surface. This means that the overlying groundwater has penetrated into the geothermal systems in the natural state and diluted the geothermal fluid as it flowed further away from the up-flow zone of Laguna Verde. This dilution trend is actually confirmed in geochemical studies (Montalvo, 1994).

4. SIMPLE LUMPED PARAMETER MODELLING

The three-dimensional, numerical reservoir simulators which have been developed to date, are complicated tools which require substantial man-time and computer power. These are generally applied during the last stage of a geothermal exploration phase, for example when a decision of constructing a new power plant is taken. One alternative to the detailed numerical modelling of complex fluid rock systems is lumped modelling. Lumped parameter modelling is probably the most powerful of the simple modelling methods. In lumped models the hydrological properties of a reservoir are lumped together in one or two quantities for several sub-volumes of the reservoir. This is analogous to the methods used for system analysis in electrical and mechanical engineering. Simple lumped parameter models can be used to predict responses of a reservoir to different future production schemes and the model gives some insight into the properties of the reservoir being simulated. In this chapter, a lumped parameter model of Axelsson (1989) is applied for the interpretation of pressure and production data from the Ahuachapán geothermal field.

4.1 The programme LUMPFIT

The lumped model, applied in this work, consists of a few capacitors or tanks that are connected by resistors. The programme LUMPFIT, which employs a non-linear, iterative, least square procedure, is used (Axelsson and Arason, 1992). An example of a three-tank model is presented in Figure 8. The tanks simulate the storage of different parts of the reservoir in question, whereas the resistors simulate the permeability. A tank in a lumped parameter model has a mass storage coefficient κ. The tank responds to a load of a liquid mass m with a pressure increase given by $p = m/\kappa$. The mass conductance of a resistor in a lumped model is σ when it transfers $q = \sigma \Delta p$ units of liquid mass per unit time at the impressed pressure differential Δp. The pressures in the tanks simulate the pressures in different parts of the reservoir, whereas production from the reservoir is simulated by withdrawal of water from only one of the tanks (Axelsson, 1989).

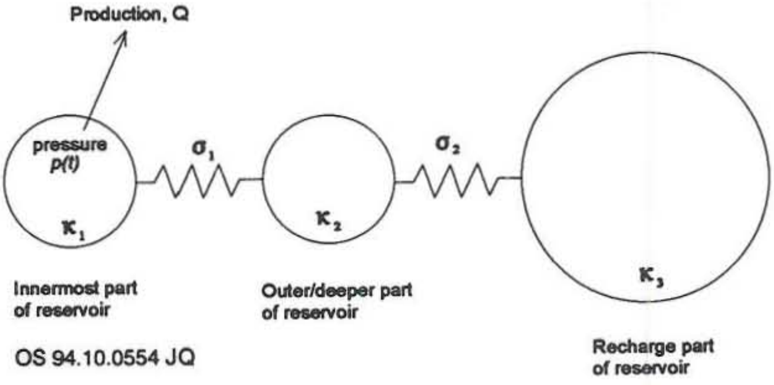

FIGURE 8: A lumped parameter model consisting of three tanks connected by resistors

Lumped models can either be open or closed. The open models are connected by a resistor to an infinitely large imaginary reservoir, which maintains a constant pressure. On the other hand, the closed, lumped models, are isolated from any external reservoir. Actual reservoirs are most generally represented by a two- or three-tank closed or open lumped parameter model (Axelsson, 1989). The pressure response, p, of a single tank open model for a constant production, Q, at times $t \geq 0$ is given by the following equation:

$$p(t) = -\frac{Q}{\sigma_1}\left(1 - e^{-\frac{\sigma_1}{\kappa_1}t}\right) \tag{1}$$

The pressure response, p, of a more general open model with N tanks, to a constant production, Q, at times $t = 0$, is given by

$$p(t) = -\sum_{j=1}^{N} Q\frac{A_j}{L_j}\left(1-e^{L_j t}\right) \tag{2}$$

The pressure response of an equivalent N tank closed model is given by the equation

$$p(t) = -\sum_{j=1}^{N-1} Q\frac{A_j}{L_j}\left(1-e^{L_j t}\right) + QBt \tag{3}$$

The coefficients A_j, L_J and B are functions of the tank storage coefficients, κ_j, and the conductance coefficients, σ_j, of the model, estimated by the LUMPFIT programme. The storage coefficients, κ_j, are related to the volumes, V_j, through the storativity, s, of a reservoir by $\kappa_j = V_j s$. The storativity is the ability of a reservoir to store fluid and release it in response to a pressure change Δp, and depends on the reservoir type. Several relations between the lumped model properties and the reservoir properties are given in Appendix III.

4.2 The Ahuachapán production history

The initial production testing of the Ahuachapán geothermal system was undertaken during 1968-1974 when about 21×10^6 tons of steam and water were extracted (Witherspoon, 1979). The pressure measurements reported during that period are average values from several downhole Kuster measurements. However, only a few of these data are currently available. At the beginning of commercial exploitation in June 1975 the pressure values reported at 200 m a.s.l were in the range of 34-35 bars. Taking into account precision of the pressure tools and the previous production, one can estimate an initial pressure for the undisturbed reservoir to be 36 bars at 200 m a.s.l.. The downhole pressure has been monitored continuously at 200 m a.s.l. in well AH-25 with Sperry Sun equipment since 1978. The pressure and mass extraction history is presented in Figure 9.

Two pressure draw down rates are evident in Figure 9. The first one, from 1975 to 1985 shows a pressure drop of 1.3 bars/year during an average net mass extraction of 409 kg/s. The second draw down period, starting in 1985, shows a pressure drop of 0.3 bars/year when the average net mass extraction is 447 kg/s. These two different draw down rates are most easily explained by changed storativity of the reservoir due to boiling. Initially, the reservoir responds to the production like a single-phase, liquid-dominated and confined system. In 1985, however, a boiling zone starts to spread out in the subsurface, leading to substantial increase in the reservoir storativity (free surface response). This conclusion is supported by measured enthalpy increase of wells AH-6, AH-17, AH-22, and AH-26 in these years.

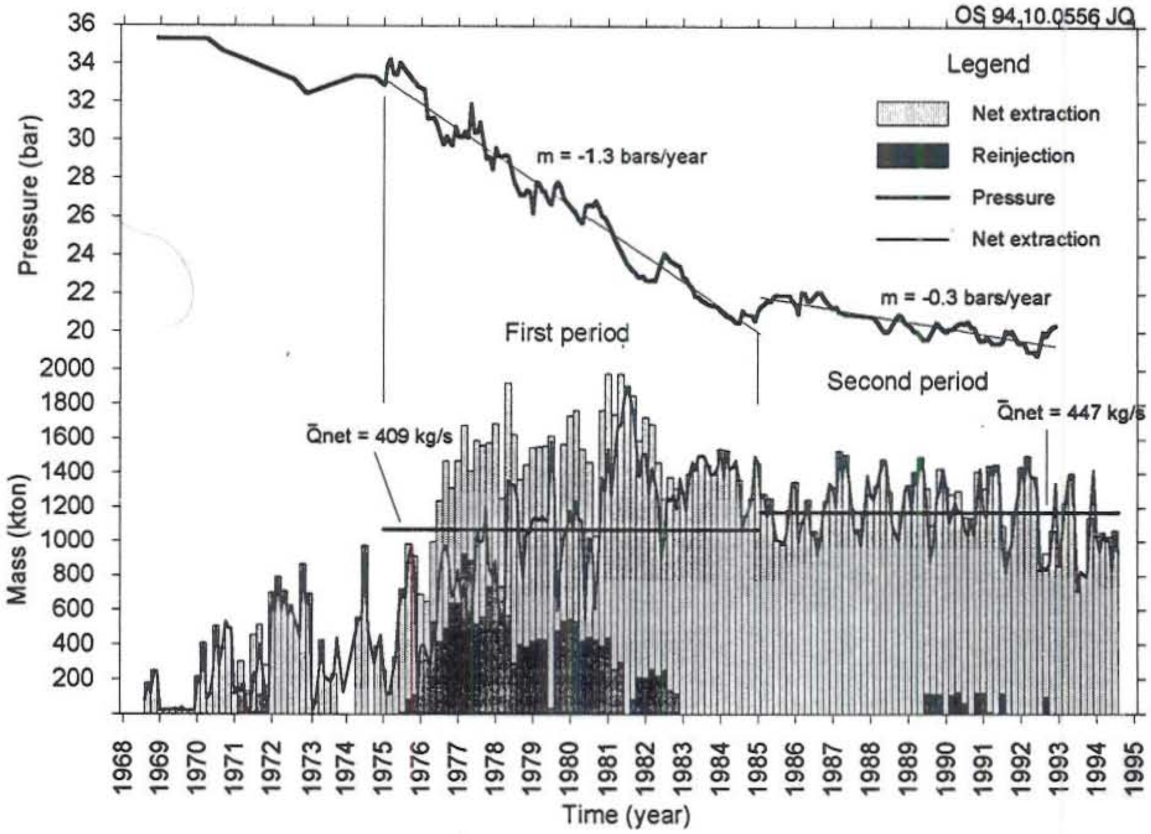

FIGURE 9: Reservoir pressure at 200 m a.s.l. and monthly mass extraction for the Ahuachapán field

4.3 A lumped parameter model for the Ahuachapán reservoir

Due to the lack of pressure data before the beginning of the commercial exploitation, only pressure data collected after 1975 were used for the lumped model inversion process. The production data in Figure 9 was simulated in two ways:

1. By inverting only pressure data collected between 1975-1985 (the liquid dominated confined reservoir response of 1.3 bars/year drawdown);

2. By inverting all the pressure data from 1975 until August 1994 (both confined and free surface reservoir response of 0.3 bars/year drawdown).

The results of the modelling with two tanks closed and open and three tanks closed are presented in Table 4 and Figure 10.

The match between observed and calculated pressure, shown in Figure 10 is good, providing a coefficient of determination of 98% and standard deviation between 0.5 and 0.7 bars. Note that the sum of the storage coefficients, κ, is 2-3 times larger for the closed models, if all the history is matched, compared to the 1975-1985 matching interval. The open model sum of storage coefficients is, on the other hand, almost the same. This difference in storativity is most likely due to an expanding boiling zone in the reservoir. Figure 10 clearly shows that without this boiling response, one would expect 5 bars lower reservoir pressure than is measured at present.

TABLE 4: Comparison of lumped parameters models for the two production periods in Ahuachapán

Period	**1975-1985**			**1975-1994**		
Number of tanks	2	2	3	2	2	3
Model type	Closed	Open	Closed	Closed	Open	Closed
κ_1 (10^3 ms^2)	11	11	10	21	13	10
κ_2	151	141	28	336	124	44
κ_3			113			359
$\Sigma\kappa_i$	162	152	150	357	137	413
σ_1 (10^{-5} ms)	74	75	97	44	64	101
σ_2		5	307		37	58
Coeff. of determ. (%)	97.36	97.36	97.32	98.27	98.4	98.49
Standard deviation (bars)	0.63	0.63	0.64	0.56	0.54	0.53

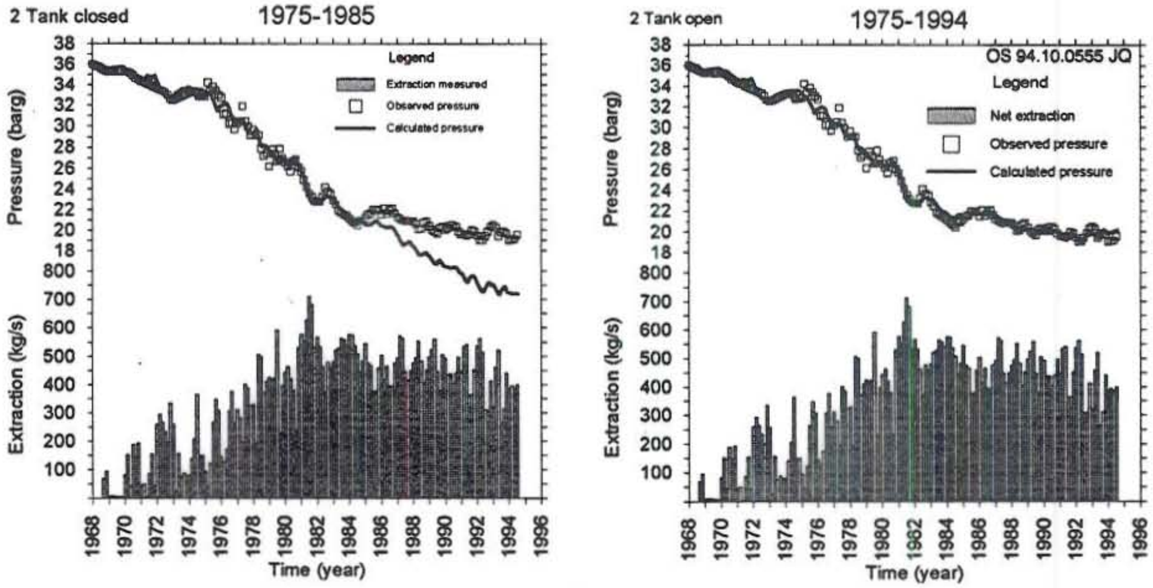

FIGURE 10: Measured and calculated pressures at 200 m a.s.l. for the two matching intervals a) 1975-1985, and b) 1975-1994

4.4 Estimation of reservoir permeability and volume

Table 5 presents estimates for the volume and permeability of the Ahuachapán geothermal reservoir using the equations shown in Appendix III. The calculations assume that the Ahuachapán reservoir as a liquid-dominated system with an average temperature of T = 235°C, fluid density of $\rho = 820$ kg/m^3, liquid compressibility of $c_w = 1.2\text{x}10^{-9}$ Pa^{-1} and rock compressibility of $c_r = 2\text{x}10^{-11}$ Pa^{-1}. The results in Table 5 show that the calculated permeability values for the one-dimensional flow (1-D) case are extremely high and three orders of magnitude higher than in the radial model (2-D). The 1-D permeability is also much higher than estimates obtained in simulation studies (LBL, 1989). The 2-D model is, therefore, considered more reliable. In general terms we can, therefore, estimate the permeability of the Ahuachapán reservoir to be in the order of 30-80 mD.

TABLE 5: Estimates of reservoir volume and permeability, assuming 10-15% porosity

Model	Reservoir volume (confined system) (km^3)		Reservoir area (free surface system) (km^2)		Permeability range (mD)			
					1-D flow ($x10^3$)		Radial flow	
	1975-1985	Total history	1975-1985	Total history	1975-1985	Total history	1975-1985	Total history
2 tanks closed	1000-1400	2000-3000	11-16	20-35	30-140	40-180	30-90	20-50
2 tanks open	900-1300	800-1200	10-15	10-13	30-140	20-100	30-90	30-70
3 tanks closed	900-1300	2500-3500	10-15	30-40	10-40	10-70	30-80	30-90

The confined system reservoir volumes presented in Table 5 are very large. If the reservoir thickness is assumed to be 2 km, a total reservoir area of 400-700 km^2 is estimated for 1975-1985, and 400 km^2 for 1975-1994. These numbers are most likely overestimated due to the 250 kg/s natural recharge which has been proposed in the natural state simulation for the Ahuachapán system (LBL, 1989). Therefore, another study where these 250 kg/s are subtracted from the total production might give more insight into the confined reservoir volume which responded to the early production in Ahuachapán.

It should be noted that the free-surface area estimate of 10-40 km^2 in Table 5 should be compared with the approximately 10 km^2 anomaly shown in Figure 5. This indicates that a free surface reservoir characterized by an expanding boiling zone might extend to areas much larger than the present 2 km^2 wellfield.

4.5 Future reservoir performance

The lumped reservoir model described in the previous chapter allows predictions of the reservoir pressure at different mass production rates in the future. Figures 11 and 12 show pressure predictions for two-tank open and closed models and mass extractions rates between 220 and 540 kg/s. The open two-tank model, which can be considered as an optimistic case, shows that a pressure equilibrium of 19 bars is obtained for extraction of 380-400 kg/s (Figure 11). The two-tank closed model should, on the other hand, be considered a pessimistic case. Figure 12 shows that if the present 19 bar reservoir pressure is to be considered as a minimum operational pressure at 200 m a.s.l. for the Ahuachapán wellfield, then the mass extraction should be restricted to 300 kg/s, for the next 10 years of production.

Finally, it should be noted that the lumped modelling presented here only simulates and predicts the pressure changes in the Ahuachapán wellfield. Temperature changes and future changes in the size of the reservoir boiling zone may change the storativity for the individual tanks and, therefore, lead to a different pressure history than predicted by the models. The results shown in Figures 11 and 12 should, therefore, be used as a reference for other simulation projects rather than a reliable estimate for the performance of the field in the future.

5. A REVISED CONCEPTUAL MODEL FOR THE AHUACHAPÁN-CHIPILAPA AREA

The conceptual model for the Ahuachapán system has undergone several changes from the initial exploration. The first models were proposed by Romagnoli et al. (1976) and Aumento et al. (1982). They limited their models to the wellfield area and suggested that the Ahuachapán and the Chipilapa fields were separate geothermal systems. In the period 1988-1989 a reservoir evaluation study of the Ahuachapán geothermal

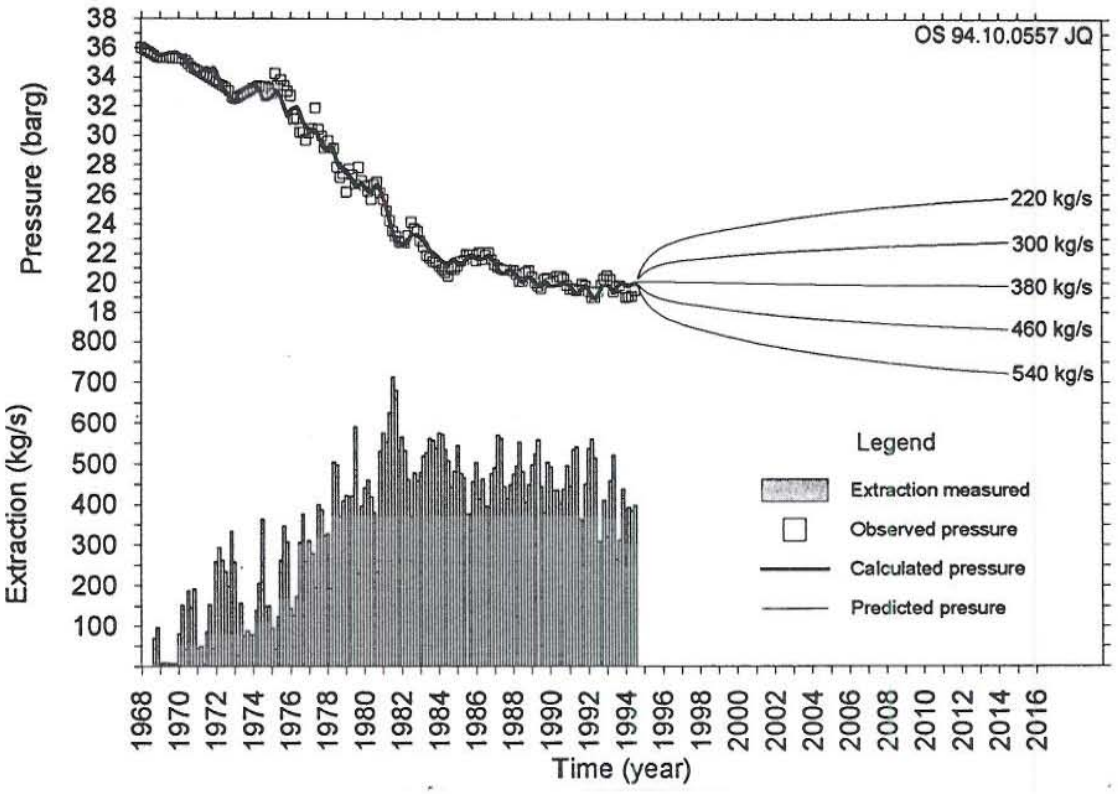

FIGURE 11: Pressure drop predictions using a 2-tank open model for the Ahuachapán reseroir

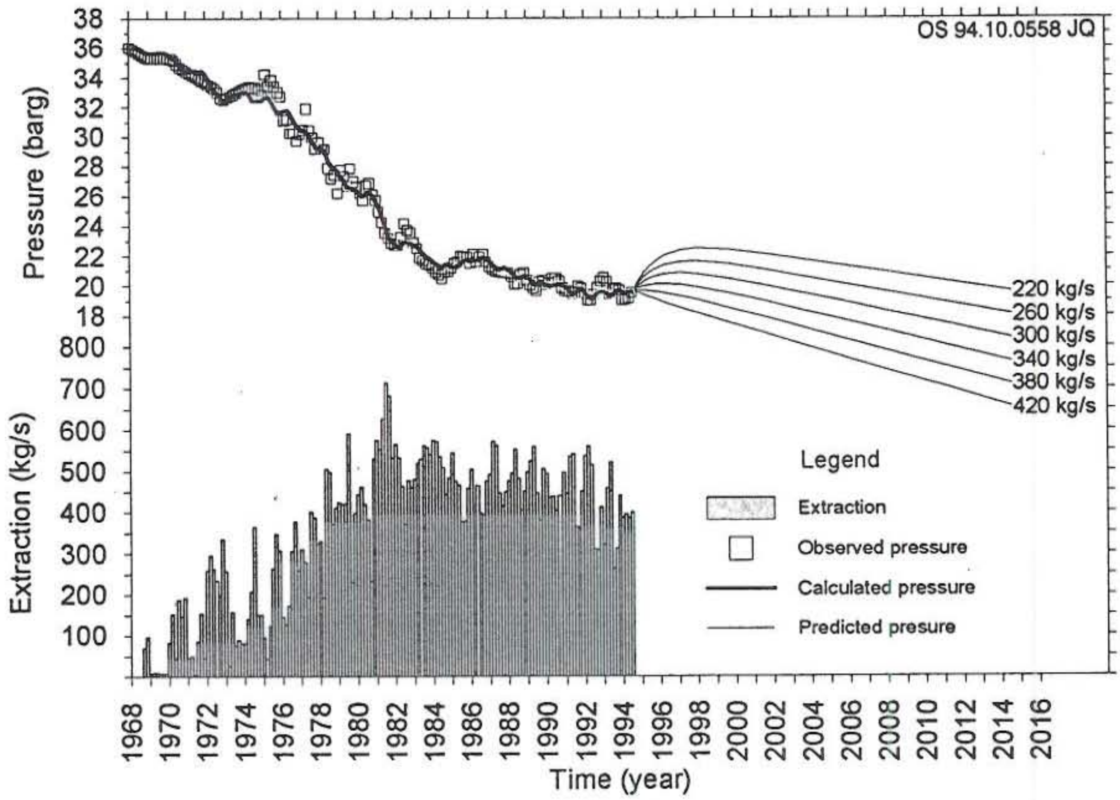

FIGURE 12: Pressure drop predictions using a 2-tank closed model for the Ahuachapán reservoir

field was carried out by the Lawrence Berkeley Laboratory (LBL, 1989). The study concentrated on the development of a hydrogeological model, the evaluation of pressure and temperature histories and reservoir simulation. As a result a conceptual model was proposed. The model states that the Ahuachapán and the Chipilapa fields are parts of the same geothermal system. The up-flow zone of this geothermal system is probably close to the Laguna Verde volcano and the main discharge zone is located in the El Salitre area.

Figure 13 shows the conceptual reservoir model proposed in this study. The major features of the model are the same as in the LBL study (1989), an up-flow zone close to the Laguna Verde volcano and a lateral outflow towards the El Salitre hot springs. Branches of this outflow are conducted laterally by the Ahuachapán andesites into the Ahuachapán and the Chipilapa wellfields. The observed pressure interference between Ahuachapán and Chipilapa confirms the hydrological connection of the two fields along with the declining flowrate from the El Salitre hot springs. The reservoir pressure in the geothermal system is relatively lower than the pressure in the overlaying groundwater zones. Some infiltration of this cooler and less saline water took place in the natural state, leading to more diluted reservoir fluids with distance from the Laguna Verde up-flow.

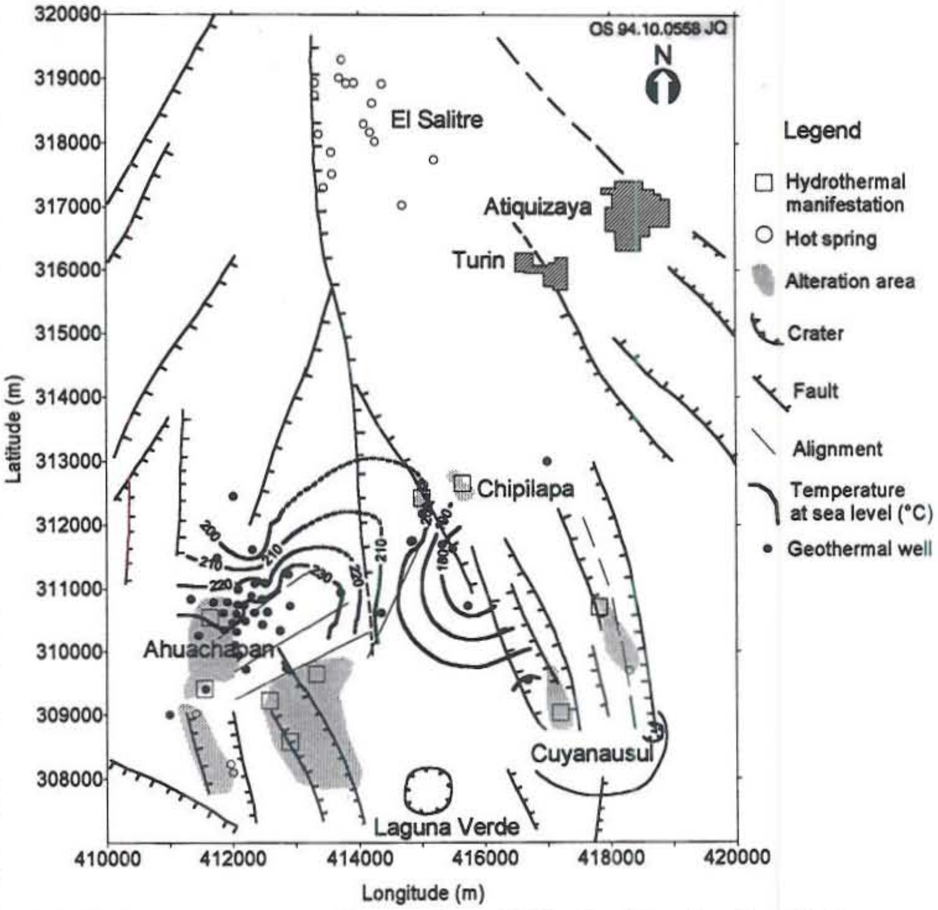

FIGURE 13: A conceptual reservoir model for the Ahuachapán-Chipilapa geothermal system

6. CONCLUSIONS

The main conclusions of the study presented in this report are the following:

1. The sub-surface temperature distribution as seen in 32 Ahuachapán wells and 8 Chipilapa wells suggests that these two fields belong to the same geothermal system. The geothermal up-flow zone for this combined system is close to the Laguna Verde volcano in the south. The geothermal fluid then flows laterally towards north-northeast.

2. The pressure history collected at 200 m a.s.l. shows that the mass production in Ahuachapán has not only led to a 17 bars pressure drawdown in the Ahuachapán wellfield but also to a 6-7 bars

drawdown in Chipilapa. This proves that there is a hydrological connection between the two fields. Production or reinjection in Chipilapa will, therefore, influence reservoir pressure in Ahuachapán.

3. Analysis of the 20 year production history of Ahuachapán together with lumped parameter modelling, shows substantial expansion of the boiling two-phase zone in the reservoir. Without this boiling process the model predicts a 5 bar lower reservoir pressure than actually is in the reservoir at present.

4 Furthermore the lumped modeling estimates a 10-30 km^2 reservoir area and permeability in the range of 30-100 mD.

5 Predictions based on the lumped parameter models indicate fairly stable reservoir pressures for the next 20 years if mass production from the field is kept at 380-400 kg/s. However, further expansion or possible collapse of the two-phase zone influences greatly the reliability of the predictions.

ACKNOWLEDGEMENTS

I want to thank all involved for having had this opportunity to participate in the United Nations University Geothermal Training Programme, especially Dr. Ingvar Birgir Fridleifsson, director of programme. Furthermore, I would like to thank Mr. Benedikt Steingrimsson and Mr. Grimur Bjornsson, my advisers, for sharing their knowledge and experience, Dr. Gudni Axelsson for his assistance with the lumped parameter models, and all the staff at Orkustofnun for their willingness to help.

NOMENCLATURE

c_w = Water compressibility [Pa^{-1}]
c_r = Rock compressibility [Pa^{-1}]
g = Acceleration of gravity [m/s^2]
H = Reservoir thickness [m]
P = Absolute pressure [Pa]
T = Temperature [°C]
H_w = Water enthalpy [J]
H_s = Steam enthalpy [J]
ϕ = Porosity
ρ_s = Steam density [kg/m^3]
ρ_t = Density of the steam-water mixture [kg/m^3]
ρ_w = Water density [kg/m^3]
ρC = Volumetric heat capacity of wet rock [J/kg m^3]

REFERENCES

Arason, P, and Bjornsson, G., 1993: *ICEBOX. User's guide.* Orkustofnun, Reykjavik.

Aumento, F., Viale, P., Choussy, M., and Santana, A., 1982: Alteration mineralogy of the Ahuachapán geothermal field. *Geoth. Res. Council, Transactions, 6,* 7-10

Axelsson, 1989: Simulation of pressure response data from geothermal reservoir by lumped parameter model. *Proceedings of the 14th Workshop on Geothermal Reservoir Engineering, Stanford University, Ca., 257-263.*

Axelsson, G., and Arason, P., 1992: *LUMPFIT, automated simulation of pressure changes in hydrological reservoirs. Version 3.1, user's guide.* Orkustofnun, Reykjavik, 32 pp.

CFG, 1992: *Geoscientific studies, evaluation report of existing data. Phase I: Chipilapa geothermal field.* CFG (Consorcio Francés de Geotermia), Project no. CEL-1684, report submitted to CEL (in Spanish), 105 pp.

Cuéllar, G., Choussy, M., and Escobar, D.,1981: Extraction-reinjection at Ahuachapán geothermal field. In: Rybach, L., and Muffler, L.J.P. (editors), *Geothermal systems. Principles and case histories.* John Wiley and Sons Ltd., Chichester, 321-336.

Einarsson, S.S., Vides R., A, and Cuéllar, G., 1976: Disposal of geothermal waste water by reinjection. *Proceedings of the 2nd United Nations Symposium on the Development and Use of Geothermal Resources, II,* 1349-1364.

Glover, R.B., 1970: Geochemical investigations of the Ahuachapán geothermal fields. In: *Survey of geothermal resources in El Salvador.* United Nations Development Programme, umpublished report.

Helgason, P., 1993: *Step by step guide to Berghiti. A user's guide.* Orkustofnun, Reykjavik, 13 pp.

IIE, 1992: *Final report of geovolcanologic study of the Ahuachapán-Chipilapa area. Final version.* IIE, Mexico, report submitted to CEL (in Spanish), 62 pp.

LBL, 1989: *The Ahuachapán geothermal field, El Salvador - Reservoir Analysis. Volume I: Text and main figures; Volume II: Appendices A through E; Volume III: Appendices F through I.* Lawrence Berkeley Laboratory, University of California, Berkeley, Ca., report LBL-26612, 201 pp + appendices.

Laky, C., Lippmann, M.J., Bodvarsson, G.S., Retana, M., and Cuellar, G., 1989: Hydrogeologic model of the Ahuachapán geothermal field, El Salvador. *Proceedings of the 14th Workshop on Geothermal Reservoir Engineering, Stanford University, USA,* 265-272.

Montalvo, F., 1994: *Chemical evolution of Ahuachapán geothermal field, El Salvador, C.A.* UNU G.T.P., Iceland, report 9, 211-236.

Nieva, D., Verma, M.P., Portugal, M.E., Santoyo, E., 1990: *Final report of geochemical studies. Chipilapa geothermal field.* IIE, Mexico, Project no. CEL-1771, report submitted to CEL, 70 pp.

Romagnoli, P., Cuéllar, G., Jiménez, M., and Ghessi G., 1976: Hydrogeological characteristics of the geothermal field of Ahuachapan, El Salvador. *Proceedings of the 2nd United Nations Symposium on the Development and Use of Geothermal Resources, 1,* 571-574.

Wieseman, G., 1975: Remarks on the geologic structure of the Republic of El Salvador, Central America. *Mitt. Geol. Palaent. Inst., University of Hamburg, 44,* 557-574.

Witherspoon, P.A., 1979: *Analysis of reservoir behavior at Ahuachapán geothermal field.* CEL, El Salvador, internal report.

APPENDIX I: GENERAL INFORMATION ON WELLS IN AHUACHAPAN AND CHIPILAPA

Well no.	Latitude (m)	Longitude (m)	Elevation (m)	Depth (m)	Drilling finished	Massflow (kg/s)	Quality	Power (MW_e)
AH-1	310741	412185	803	1195	04.Jun.68	55	0.1	3.3
AH-2	311229	412886	808	1200	06.Sep.73			
AH-3	310726	412916	856	802	01.Jun.73			
AH-4	310835	412470	812	788	04.Aug.72			
AH-5	311081	412358	789	957	30.Jun.70			
AH-6	310791	411921	783	591	24.Feb.70	16	0.78	4.4
AH-7	310342	411868	805	950	04.Jun.70	40	0.13	3.1
AH-8	310251	411458	811	988	18.Sep.72			
AH-9	309408	411573	871	1424	27.Mar.70			
AH-10	312448	412015	724	1524	18.May 70			
AH-11	311619	412319	759	943	11.Jan.73			
AH-12	311494	411758	759	1003	16.Mar.73			
AH-13	310428	412480	860	831	14.Jan.74			
AH-14	310939	413706	822	1056	12.May 74			
AH-15	310834	411334	773	704	19.Oct.74			
AH-16	309948	412106	869	1006	05.Aug.74			
AH-17	310782	411697	773	1200	30.Aug.76	15	1	6.1
AH-18	309745	412852	926	1256	24.May 77			
AH-19	310332	412759	873	1416	28.Feb.78	47	0.14	3.5
AH-20	310986	412087	793	850	20.Dec.74	61	0.2	5.8
AH-21	310601	412059	795	849	04.Mar.75	86	0.15	7.1
AH-22	310632	412559	843	660	21.Apr.75	18	0.34	2.6
AH-23	310621	412350	825	924	10.Sep.77	35	0.22	4.5
AH-24	310616	411852	783	850	23.Jun.75	36	0.15	3
AH-25	310887	412304	799	943	27.Aug.75			
AH-26	310750	412080	791	804	30.Oct.75	19	0.43	2.8
AH-27	310313	412067	822	800	29.Apr.78	58	0.25	7.4
AH-28	310490	412207	829	1000	29.Nov.78	58	0.13	4.6
AH-29	311097	412511	795	1198	11.Feb.76			
AH-30	310461	411990	804	1200	17.Feb.79			
AH-31	310098	412041	845	1502	29.Sep.81	79	0.14	6.1
AH-32	309721	412210	882	1504	31.Dec.81	71	0.14	5.4
CH-1	311747	414828	758	985	1968			
CHe-1	311700	415320	750	325	1968			
CH-7	311634	415491	766	1500	13.Jul.89			
CH-7bis	311760	414851	758	1348	26.Feb.91	19	0.21	
CH-8	310731	415734	914	2553	24.Feb.90			
CH-9	312174	415006	741	1999	25.Nov.90	46	0.11	
CH-A	309544	416688	1149	2700	10.May 92			
CH-D	310620	414351	869	1500	04.Jun.93	19	0.26	

APPENDIX II: MEASURED TEMPERATURE PROFILES AND ESTIMATED FORMATION TEMPERATURE FOR THE AHUACHAPAN AND CHIPILAPA WELLS

Measured temperature profiles are shown with solid lines, estimated formation temperature with dashed lines.

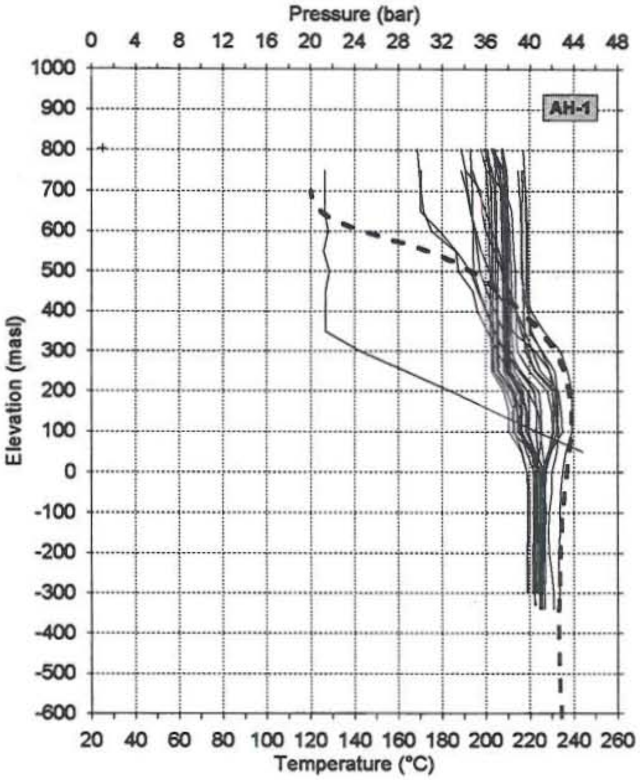

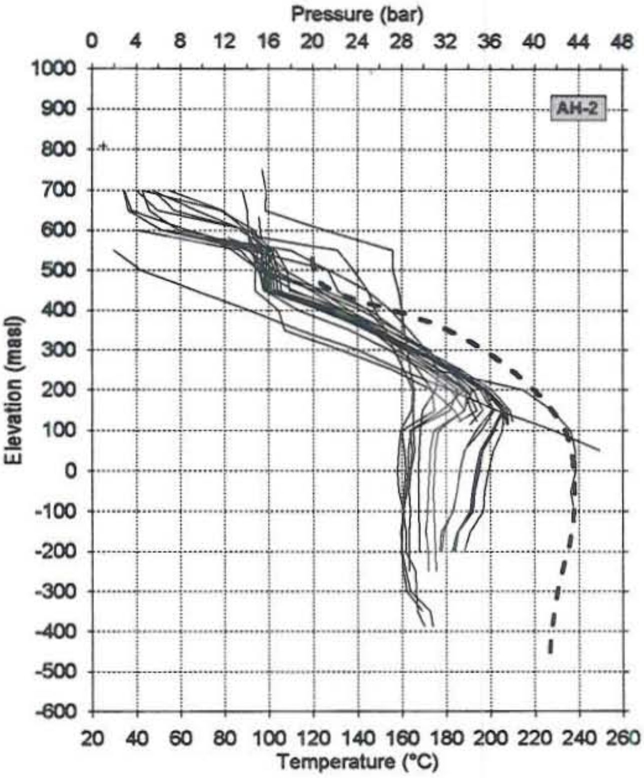

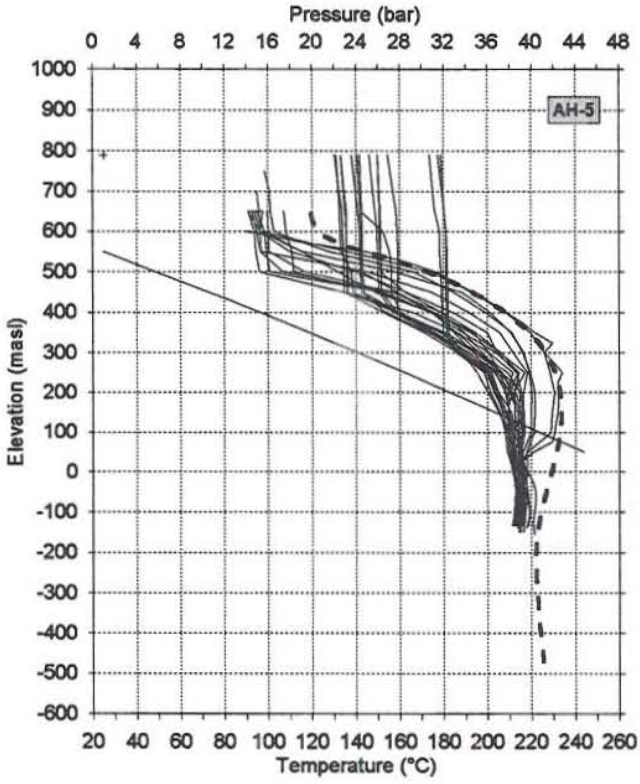

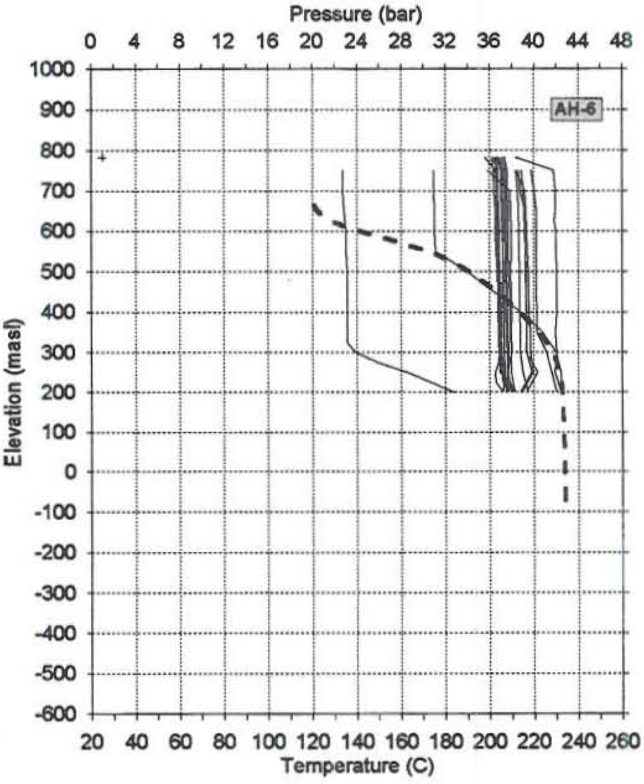

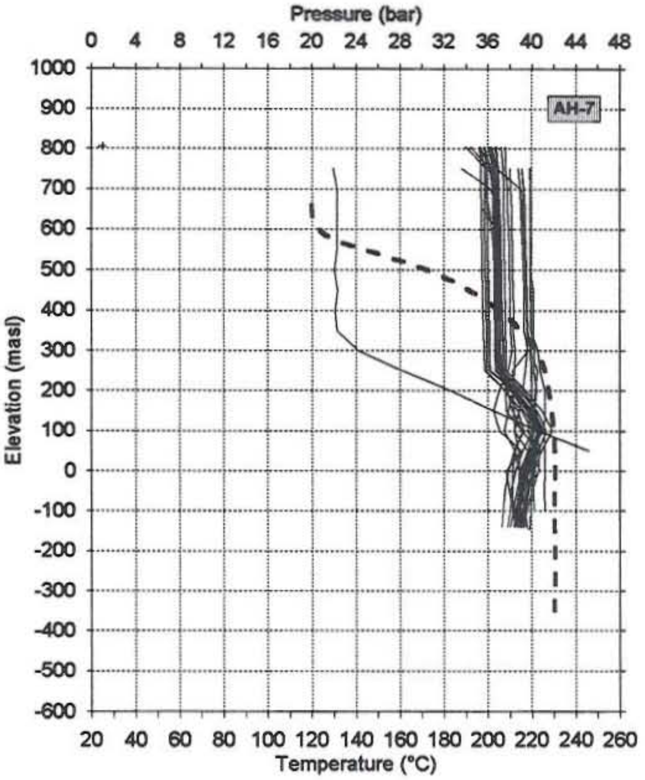
Pressure (bar)
0 4 8 12 16 20 24 28 32 36 40 44 48
AH-7
Elevation (masl)
1000 900 800 700 600 500 400 300 200 100 0 -100 -200 -300 -400 -500 -600
20 40 60 80 100 120 140 160 180 200 220 240 260
Temperature (°C)

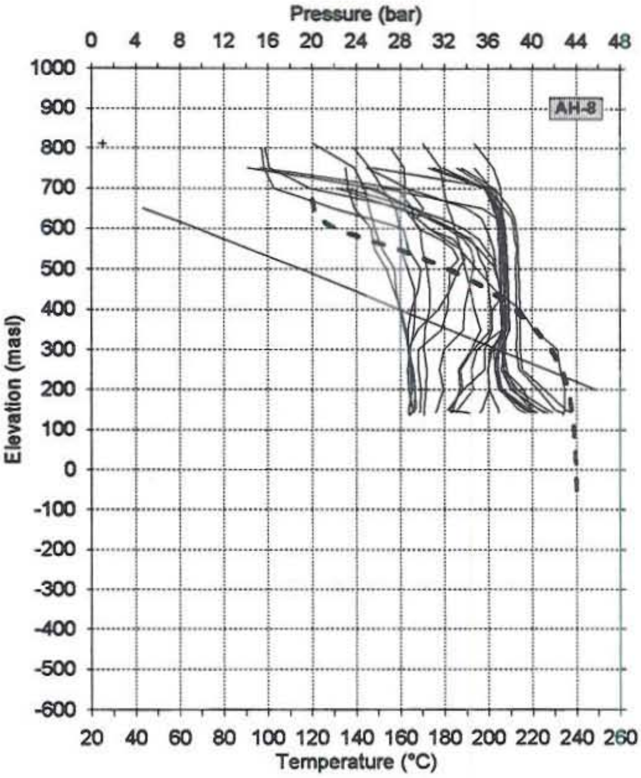
Pressure (bar)
0 4 8 12 16 20 24 28 32 36 40 44 48
AH-8
Elevation (masl)
1000 900 800 700 600 500 400 300 200 100 0 -100 -200 -300 -400 -500 -600
20 40 60 80 100 120 140 160 180 200 220 240 260
Temperature (°C)

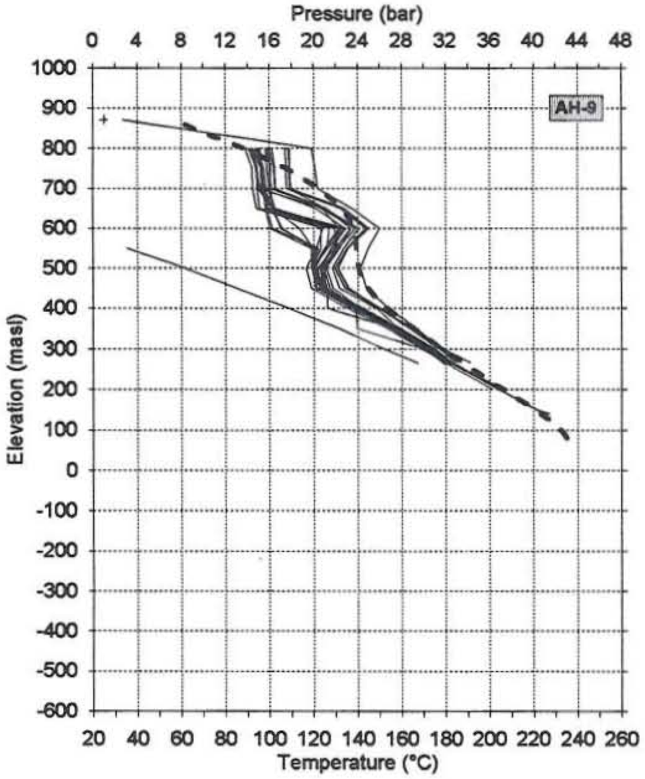
Pressure (bar)
0 4 8 12 16 20 24 28 32 36 40 44 48
AH-9
Elevation (masl)
1000 900 800 700 600 500 400 300 200 100 0 -100 -200 -300 -400 -500 -600
20 40 60 80 100 120 140 160 180 200 220 240 260
Temperature (°C)

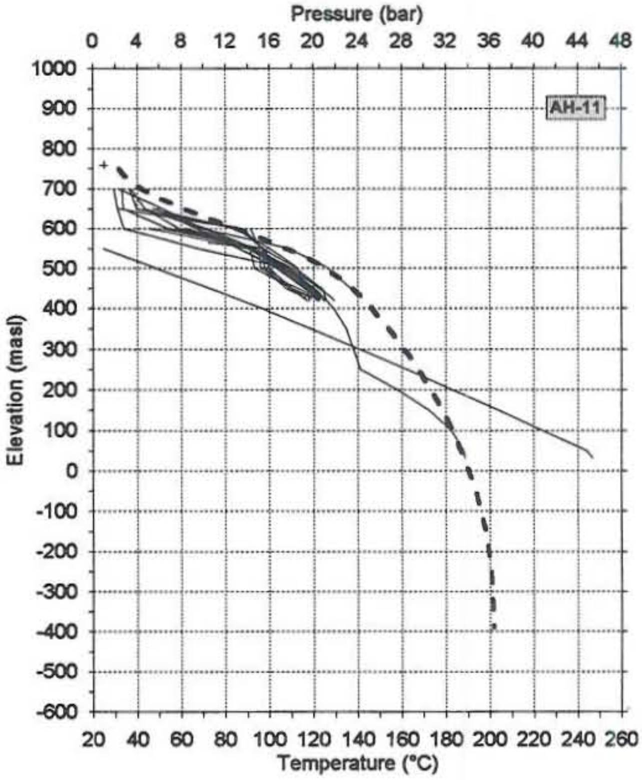
Pressure (bar)
0 4 8 12 16 20 24 28 32 36 40 44 48
AH-11
Elevation (masl)
1000 900 800 700 600 500 400 300 200 100 0 -100 -200 -300 -400 -500 -600
20 40 60 80 100 120 140 160 180 200 220 240 260
Temperature (°C)

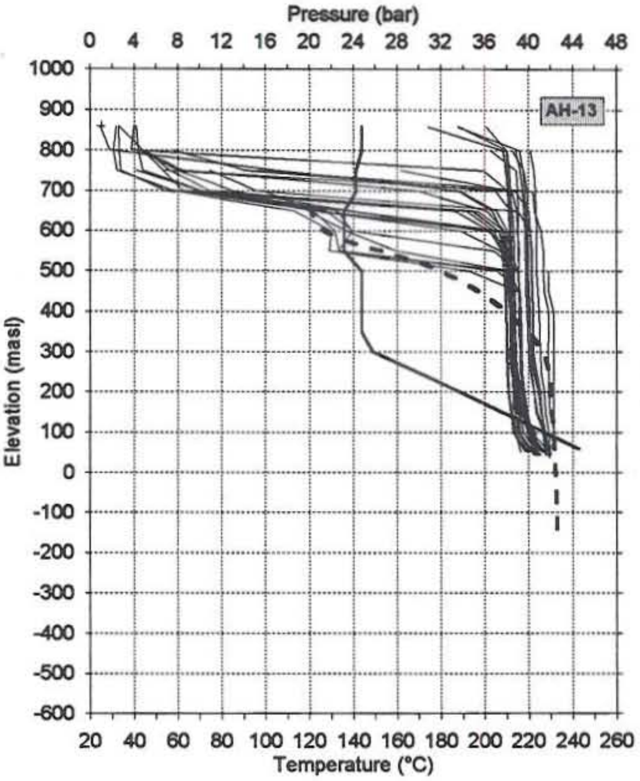
Pressure (bar)
0 4 8 12 16 20 24 28 32 36 40 44 48
AH-13
Elevation (masl)
1000 900 800 700 600 500 400 300 200 100 0 -100 -200 -300 -400 -500 -600
20 40 60 80 100 120 140 160 180 200 220 240 260
Temperature (°C)

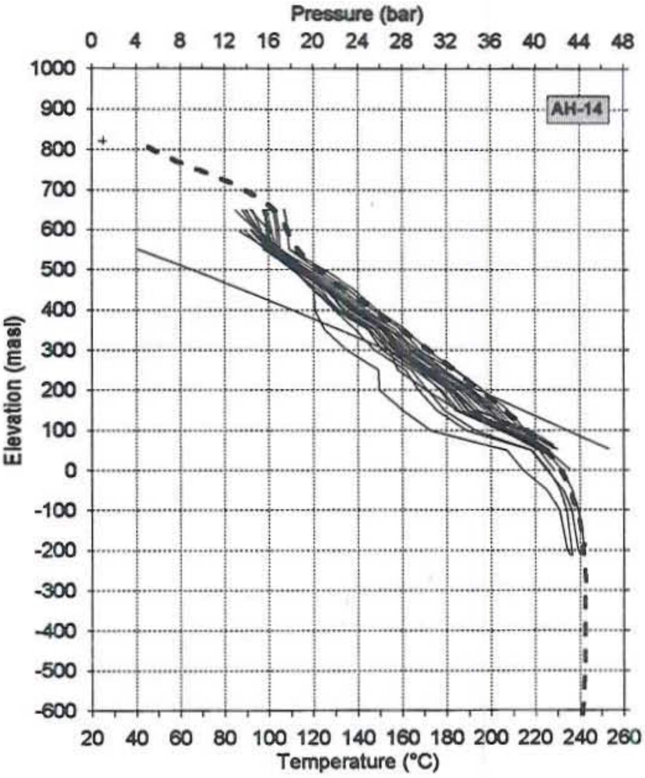
Pressure (bar)
0 4 8 12 16 20 24 28 32 36 40 44 48
AH-14
Elevation (masl)
1000 900 800 700 600 500 400 300 200 100 0 -100 -200 -300 -400 -500 -600
20 40 60 80 100 120 140 160 180 200 220 240 260
Temperature (°C)

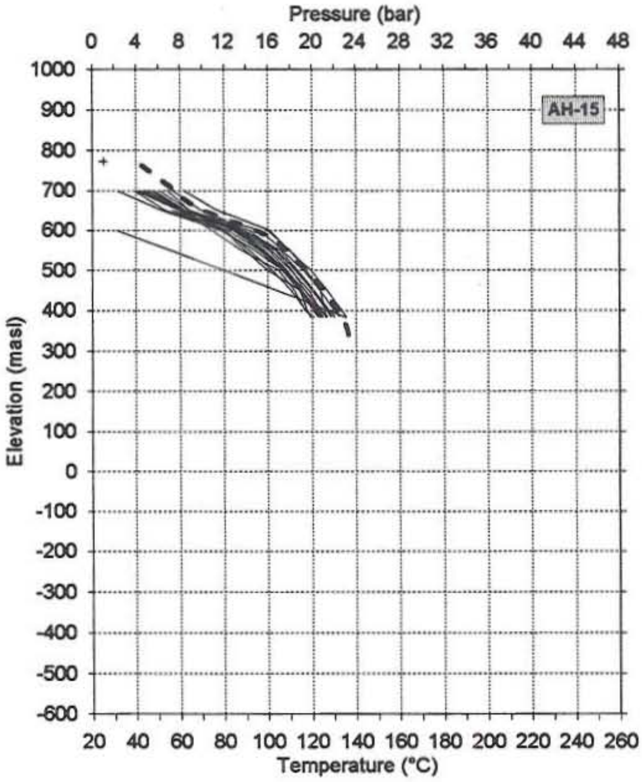
Pressure (bar)
0 4 8 12 16 20 24 28 32 36 40 44 48
AH-15
Elevation (masl)
1000 900 800 700 600 500 400 300 200 100 0 -100 -200 -300 -400 -500 -600
20 40 60 80 100 120 140 160 180 200 220 240 260
Temperature (°C)

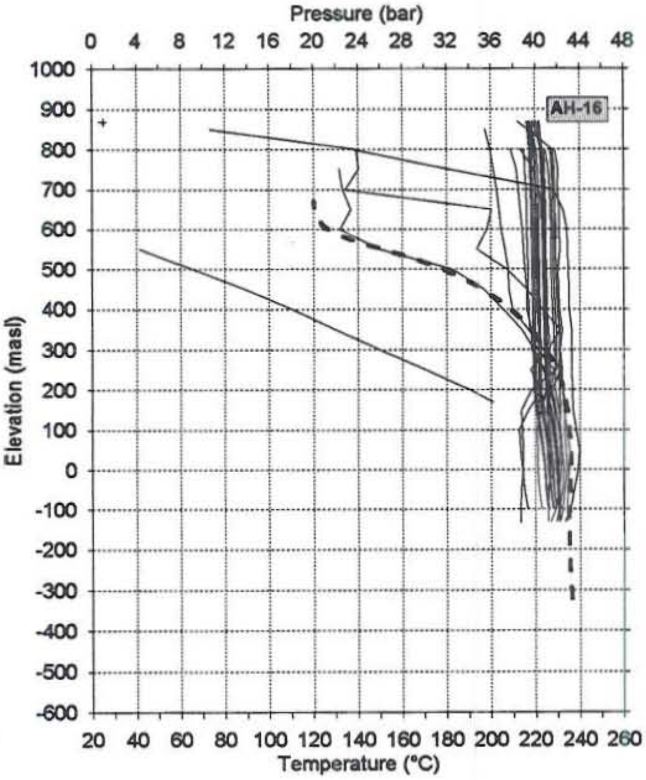
Pressure (bar)
0 4 8 12 16 20 24 28 32 36 40 44 48
AH-16
Elevation (masl)
1000 900 800 700 600 500 400 300 200 100 0 -100 -200 -300 -400 -500 -600
20 40 60 80 100 120 140 160 180 200 220 240 260
Temperature (°C)

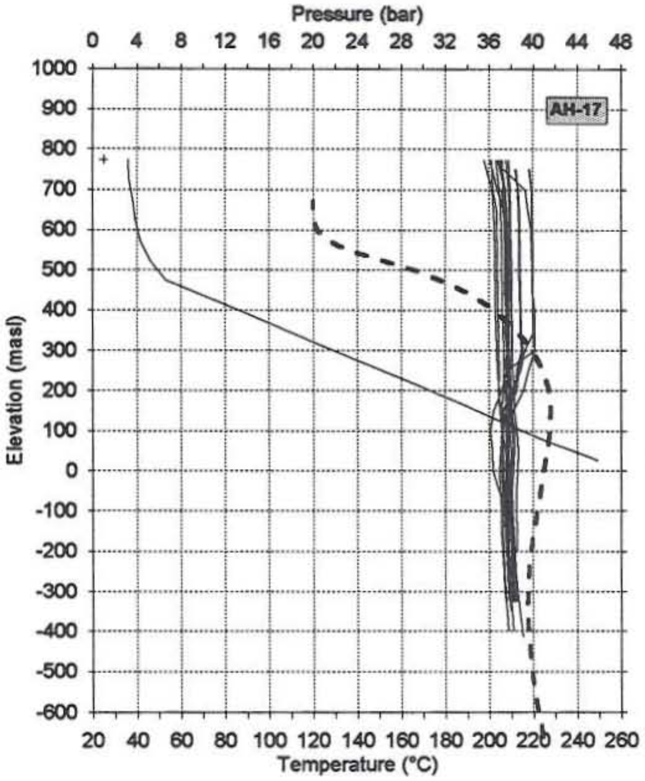
Pressure (bar)
0 4 8 12 16 20 24 28 32 36 40 44 48
AH-17
Elevation (masl)
1000 900 800 700 600 500 400 300 200 100 0 -100 -200 -300 -400 -500 -600
20 40 60 80 100 120 140 160 180 200 220 240 260
Temperature (°C)

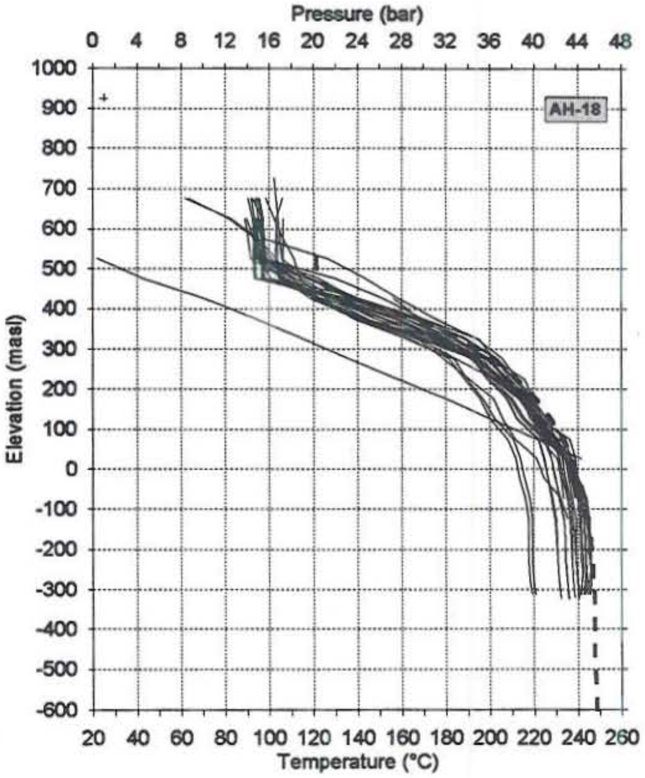
Pressure (bar)
0 4 8 12 16 20 24 28 32 36 40 44 48
AH-18
Elevation (masl)
1000 900 800 700 600 500 400 300 200 100 0 -100 -200 -300 -400 -500 -600
20 40 60 80 100 120 140 160 180 200 220 240 260
Temperature (°C)

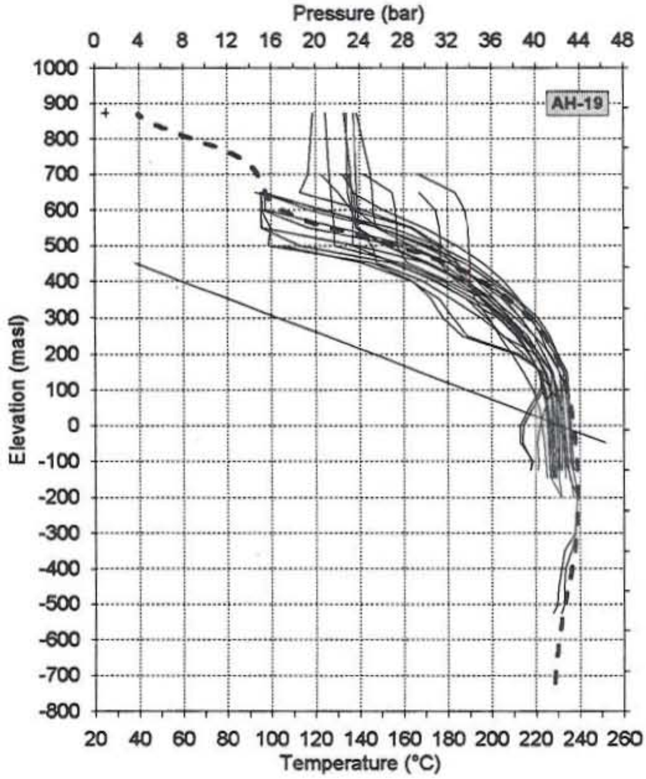
Pressure (bar)
0 4 8 12 16 20 24 28 32 36 40 44 48
AH-19
Elevation (masl)
1000 900 800 700 600 500 400 300 200 100 0 -100 -200 -300 -400 -500 -600 -700 -800
20 40 60 80 100 120 140 160 180 200 220 240 260
Temperature (°C)

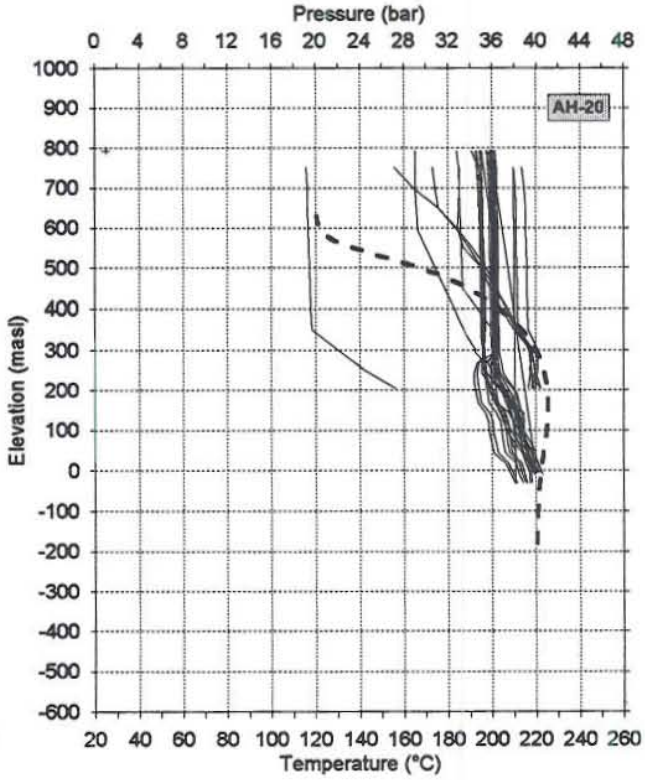
Pressure (bar)
0 4 8 12 16 20 24 28 32 36 40 44 48
AH-20
Elevation (masl)
1000 900 800 700 600 500 400 300 200 100 0 -100 -200 -300 -400 -500 -600
20 40 60 80 100 120 140 160 180 200 220 240 260
Temperature (°C)

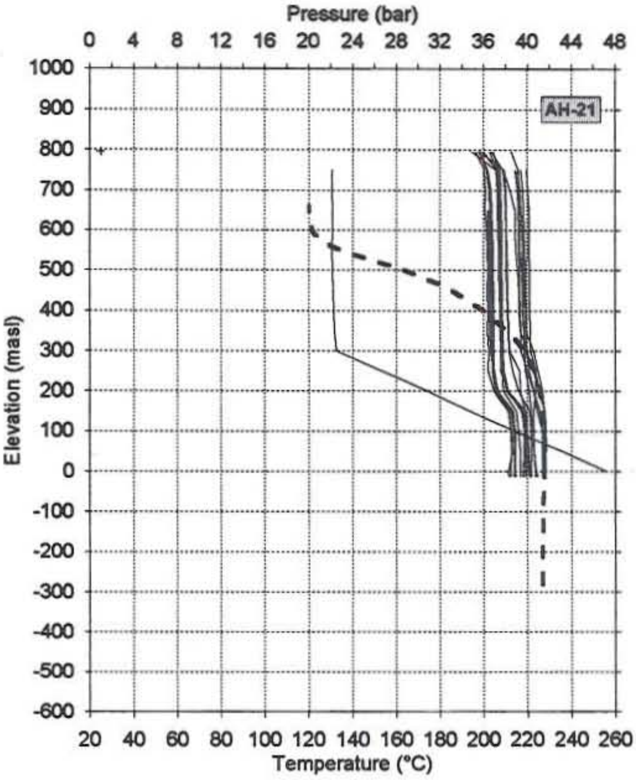
Pressure (bar)
0 4 8 12 16 20 24 28 32 36 40 44 48
AH-21
Elevation (masl)
1000 900 800 700 600 500 400 300 200 100 0 -100 -200 -300 -400 -500 -600
20 40 60 80 100 120 140 160 180 200 220 240 260
Temperature (°C)

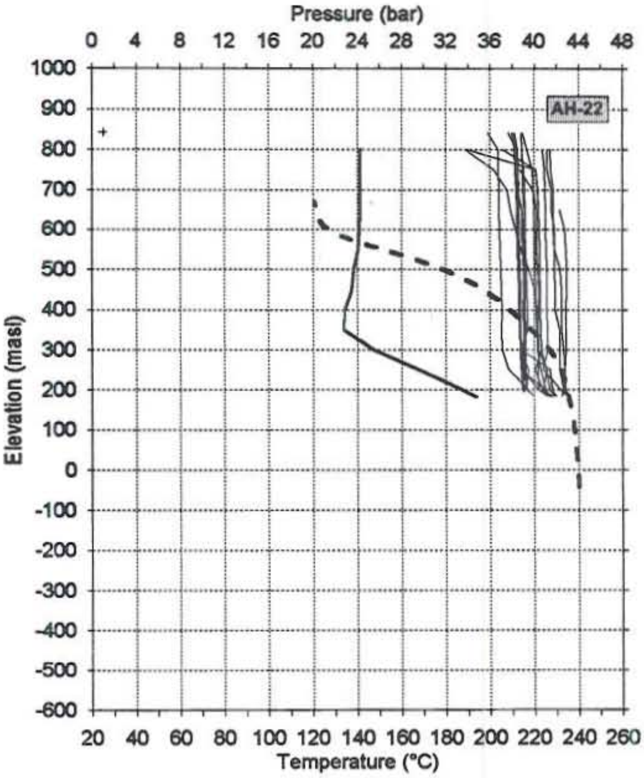
Pressure (bar)
0 4 8 12 16 20 24 28 32 36 40 44 48
AH-22
Elevation (masl)
1000 900 800 700 600 500 400 300 200 100 0 -100 -200 -300 -400 -500 -600
20 40 60 80 100 120 140 160 180 200 220 240 260
Temperature (°C)

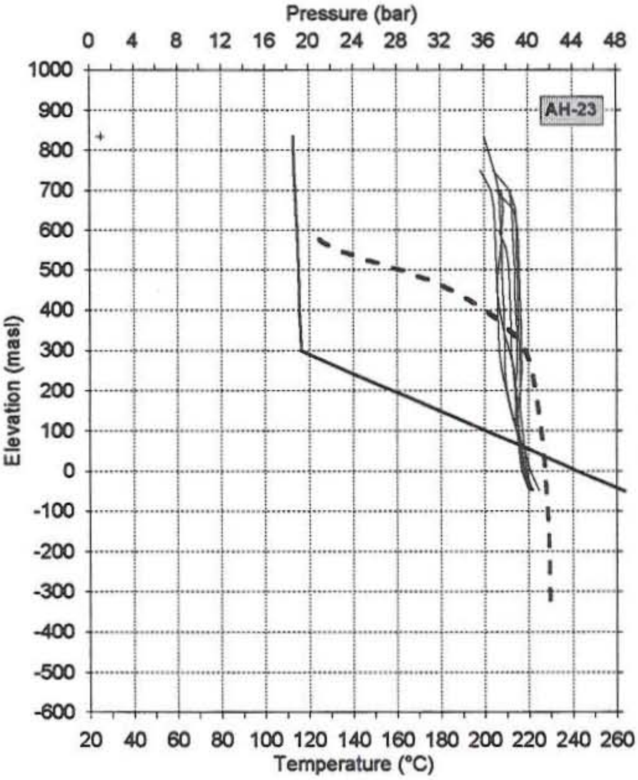
Pressure (bar)
0 4 8 12 16 20 24 28 32 36 40 44 48
AH-23
Elevation (masl)
1000 900 800 700 600 500 400 300 200 100 0 -100 -200 -300 -400 -500 -600
20 40 60 80 100 120 140 160 180 200 220 240 260
Temperature (°C)

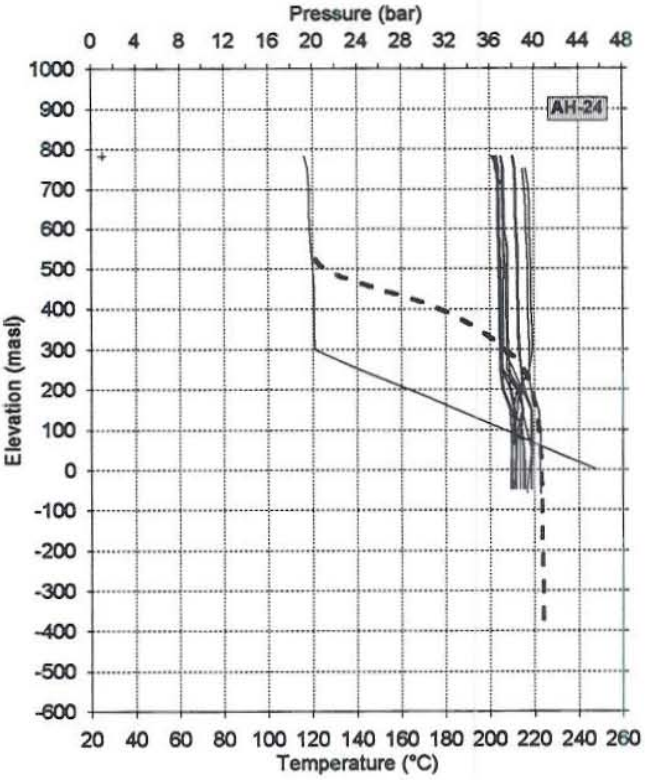
Pressure (bar)
0 4 8 12 16 20 24 28 32 36 40 44 48
AH-24
Elevation (masl)
1000 900 800 700 600 500 400 300 200 100 0 -100 -200 -300 -400 -500 -600
20 40 60 80 100 120 140 160 180 200 220 240 260
Temperature (°C)

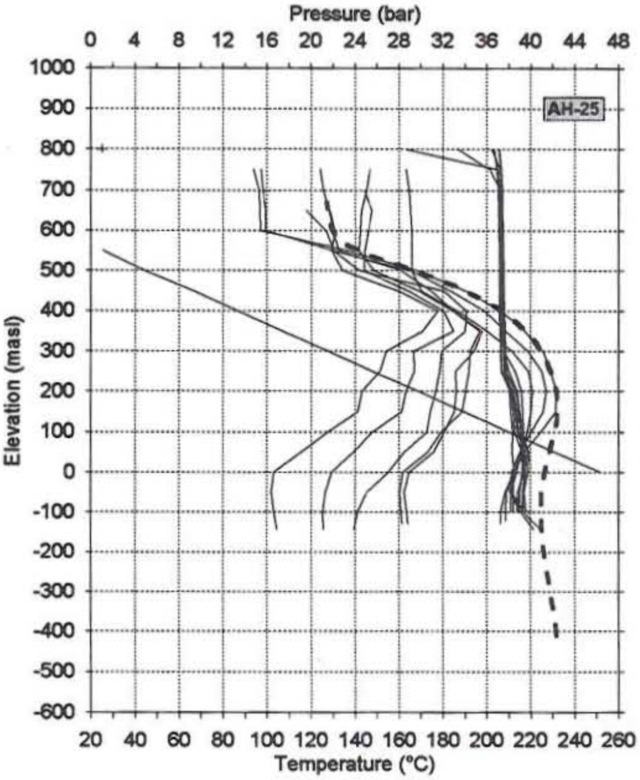
Pressure (bar)
0 4 8 12 16 20 24 28 32 36 40 44 48
AH-25
Elevation (masl)
1000 900 800 700 600 500 400 300 200 100 0 -100 -200 -300 -400 -500 -600
20 40 60 80 100 120 140 160 180 200 220 240 260
Temperature (°C)

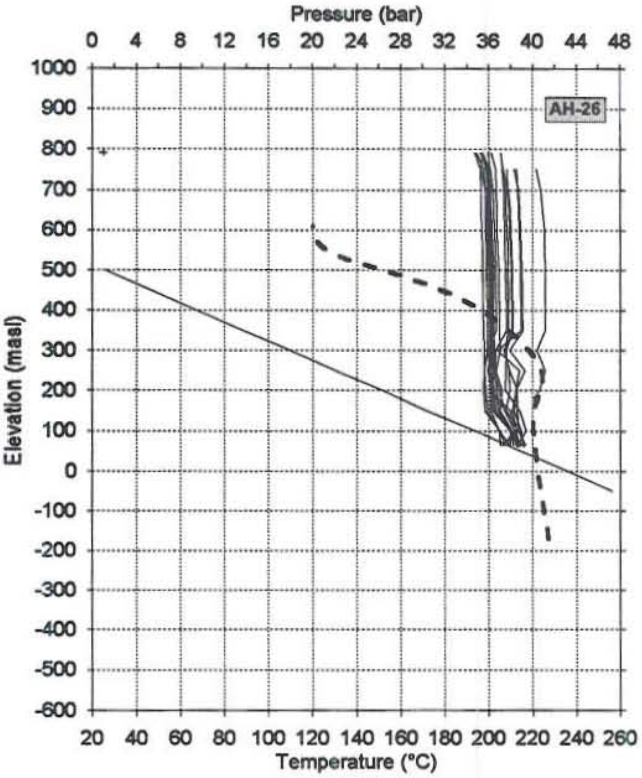
Pressure (bar)
0 4 8 12 16 20 24 28 32 36 40 44 48
AH-26
Elevation (masl)
1000 900 800 700 600 500 400 300 200 100 0 -100 -200 -300 -400 -500 -600
20 40 60 80 100 120 140 160 180 200 220 240 260
Temperature (°C)

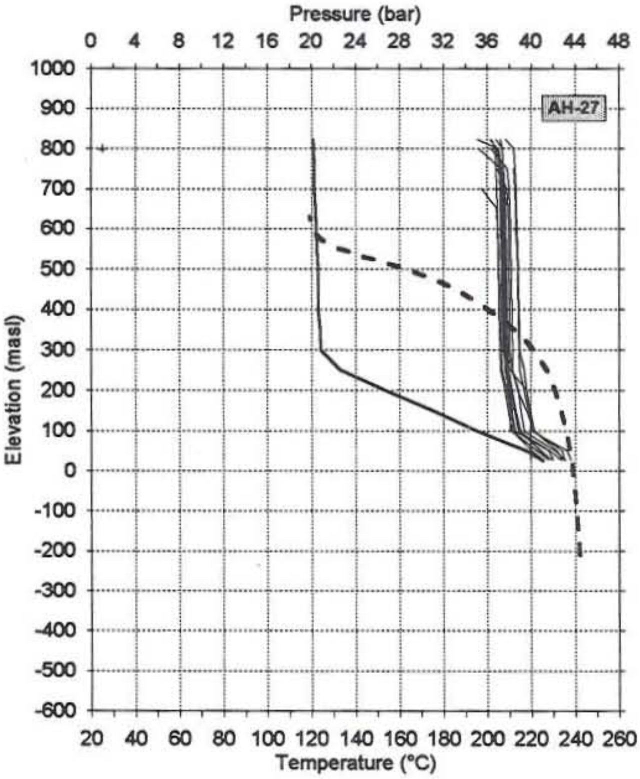
Pressure (bar)
0 4 8 12 16 20 24 28 32 36 40 44 48
AH-27
Elevation (masl)
1000 900 800 700 600 500 400 300 200 100 0 -100 -200 -300 -400 -500 -600
20 40 60 80 100 120 140 160 180 200 220 240 260
Temperature (°C)

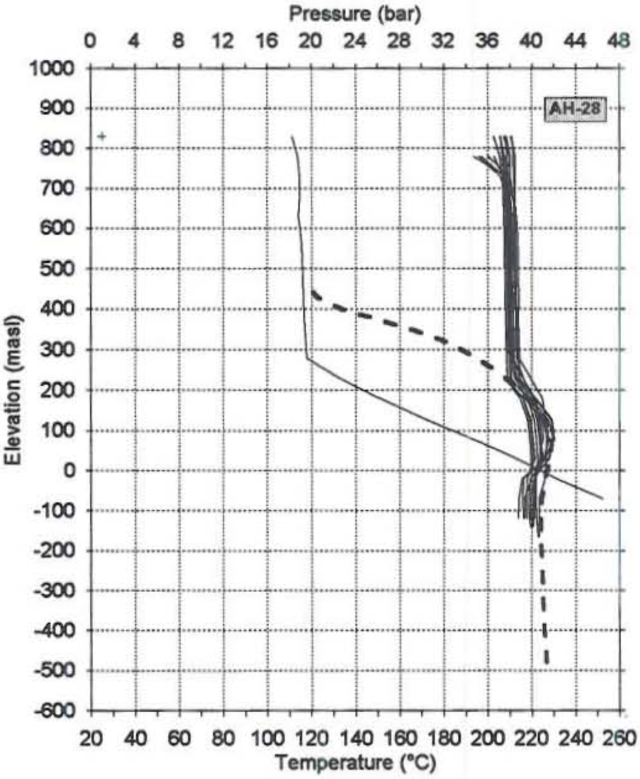
Pressure (bar)
0 4 8 12 16 20 24 28 32 36 40 44 48
AH-28
Elevation (masl)
1000 900 800 700 600 500 400 300 200 100 0 -100 -200 -300 -400 -500 -600
20 40 60 80 100 120 140 160 180 200 220 240 260
Temperature (°C)

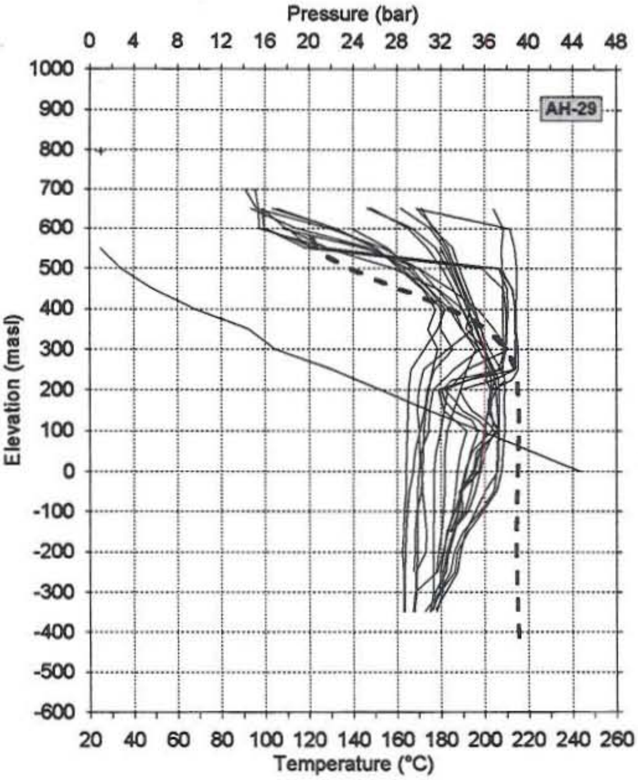
Pressure (bar)
0 4 8 12 16 20 24 28 32 36 40 44 48
AH-29
Elevation (masl)
1000 900 800 700 600 500 400 300 200 100 0 -100 -200 -300 -400 -500 -600
20 40 60 80 100 120 140 160 180 200 220 240 260
Temperature (°C)

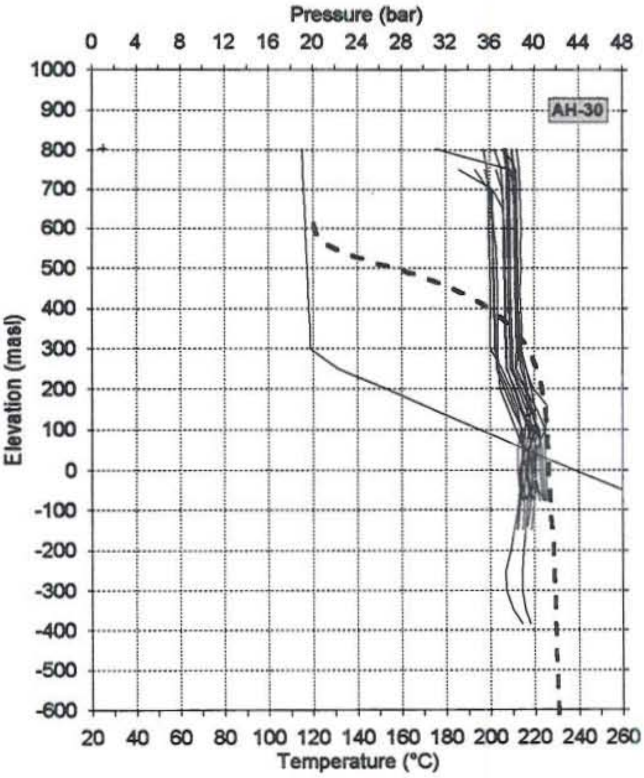
Pressure (bar)
0 4 8 12 16 20 24 28 32 36 40 44 48
AH-30
Elevation (masl)
1000 900 800 700 600 500 400 300 200 100 0 -100 -200 -300 -400 -500 -600
20 40 60 80 100 120 140 160 180 200 220 240 260
Temperature (°C)

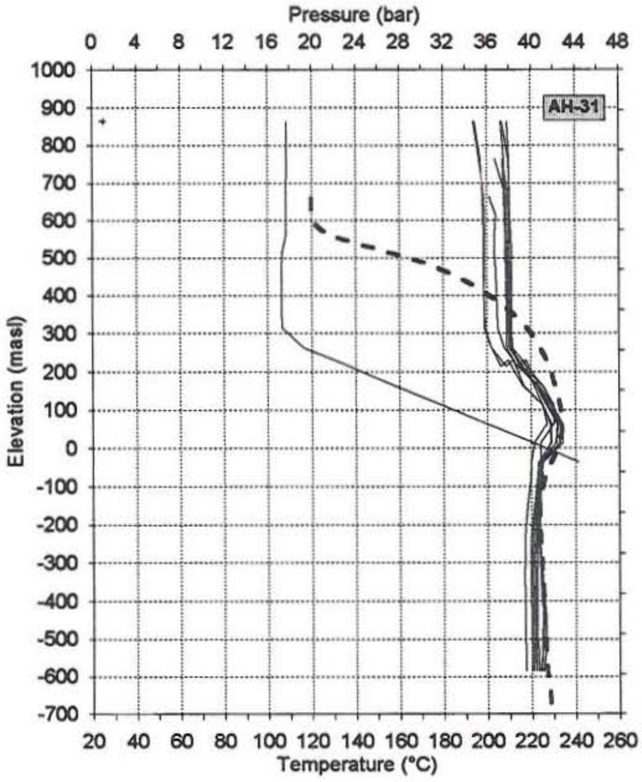
Pressure (bar)
0 4 8 12 16 20 24 28 32 36 40 44 48
AH-31
Elevation (masl)
1000 900 800 700 600 500 400 300 200 100 0 -100 -200 -300 -400 -500 -600 -700
20 40 60 80 100 120 140 160 180 200 220 240 260
Temperature (°C)

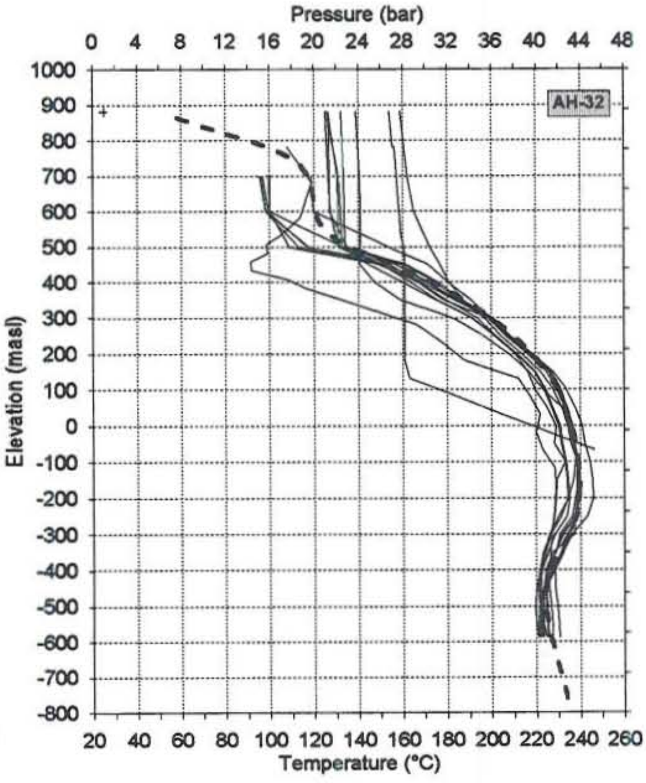
Pressure (bar)
0 4 8 12 16 20 24 28 32 36 40 44 48
AH-32
Elevation (masl)
1000 900 800 700 600 500 400 300 200 100 0 -100 -200 -300 -400 -500 -600 -700 -800
20 40 60 80 100 120 140 160 180 200 220 240 260
Temperature (°C)

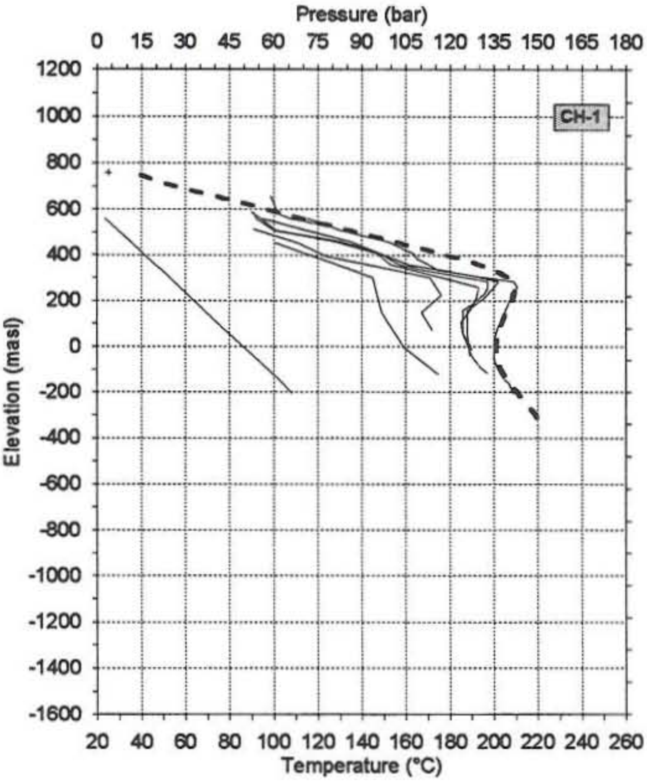
Pressure (bar)
0 15 30 45 60 75 90 105 120 135 150 165 180
CH-1
Elevation (masl)
1200 1000 800 600 400 200 0 -200 -400 -600 -800 -1000 -1200 -1400 -1600
20 40 60 80 100 120 140 160 180 200 220 240 260
Temperature (°C)

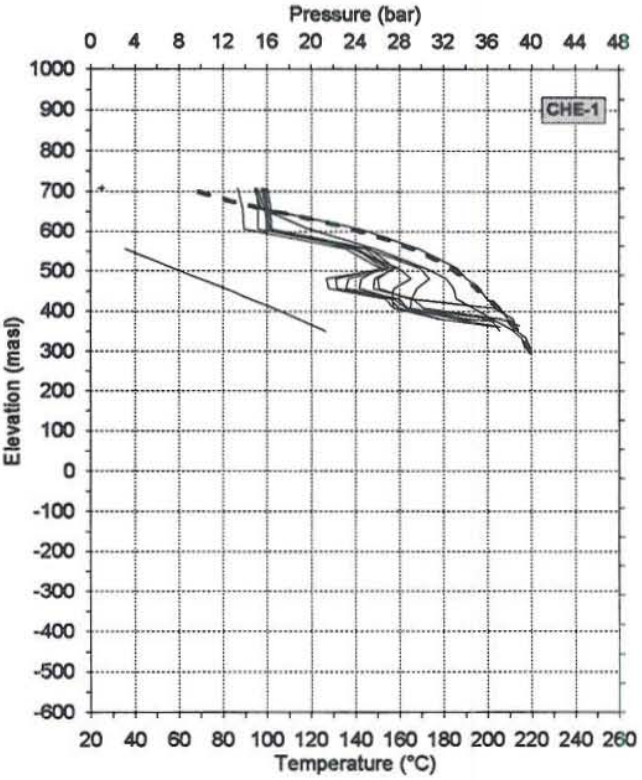
Pressure (bar)
0 4 8 12 16 20 24 28 32 36 40 44 48
CHE-1
Elevation (masl)
1000 900 800 700 600 500 400 300 200 100 0 -100 -200 -300 -400 -500 -600
20 40 60 80 100 120 140 160 180 200 220 240 260
Temperature (°C)


Pressure (bar)
0 15 30 45 60 75 90 105 120 135 150 165 180
CH-7
Elevation (masl)
1200 1000 800 600 400 200 0 -200 -400 -600 -800 -1000 -1200 -1400 -1600
20 40 60 80 100 120 140 160 180 200 220 240 260
Temperature (°C)

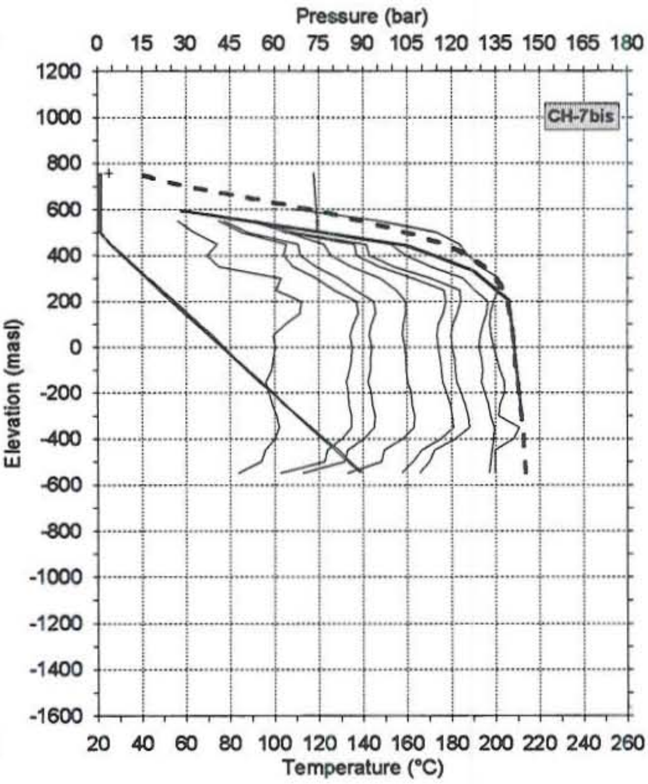
Pressure (bar)
0 15 30 45 60 75 90 105 120 135 150 165 180
CH-7bis
Elevation (masl)
1200 1000 800 600 400 200 0 -200 -400 -600 -800 -1000 -1200 -1400 -1600
20 40 60 80 100 120 140 160 180 200 220 240 260
Temperature (°C)

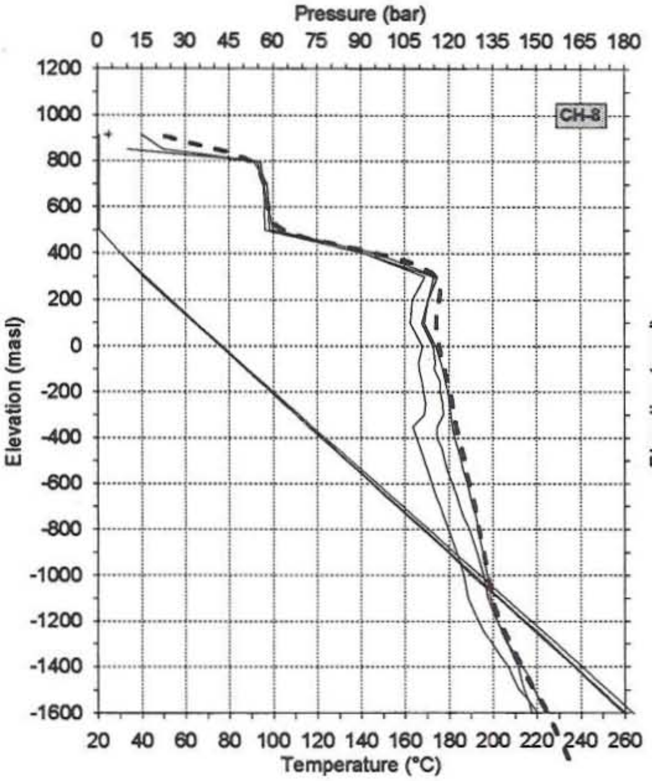
Pressure (bar)
0 15 30 45 60 75 90 105 120 135 150 165 180
CH-8
Elevation (masl)
1200 1000 800 600 400 200 0 -200 -400 -600 -800 -1000 -1200 -1400 -1600
20 40 60 80 100 120 140 160 180 200 220 240 260
Temperature (°C)

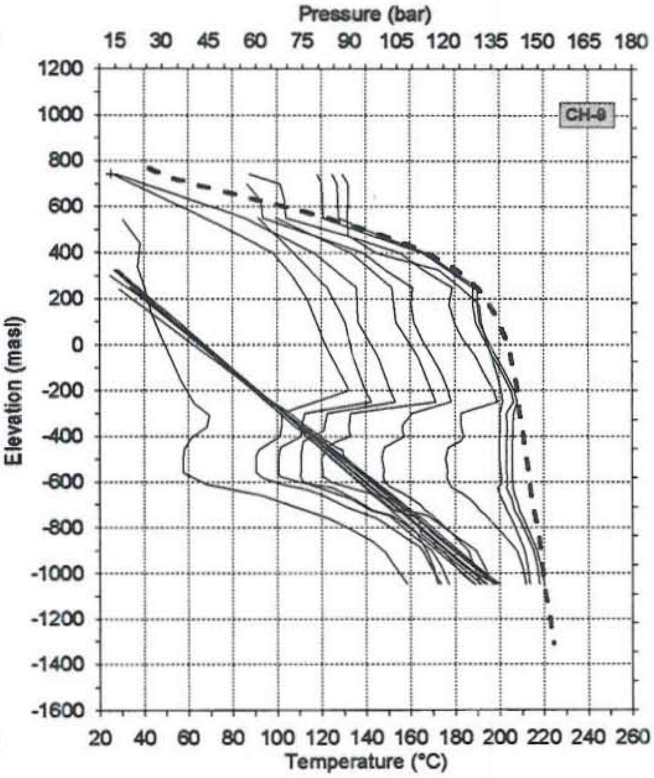
Pressure (bar)
15 30 45 60 75 90 105 120 135 150 165 180
CH-9
Elevation (masl)
1200 1000 800 600 400 200 0 -200 -400 -600 -800 -1000 -1200 -1400 -1600
20 40 60 80 100 120 140 160 180 200 220 240 260
Temperature (°C)

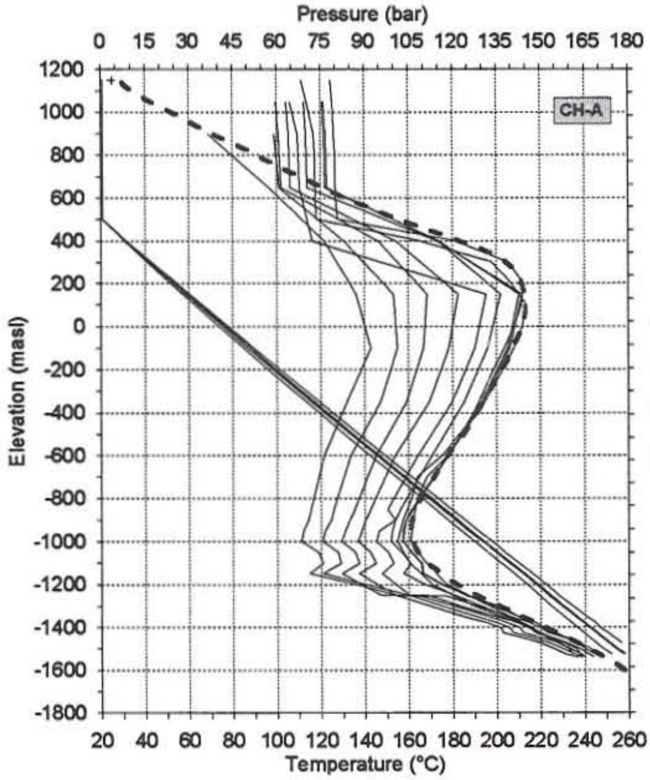
Pressure (bar)
0 15 30 45 60 75 90 105 120 135 150 165 180
CH-A
Elevation (masl)
1200 1000 800 600 400 200 0 -200 -400 -600 -800 -1000 -1200 -1400 -1600 -1800
20 40 60 80 100 120 140 160 180 200 220 240 260
Temperature (°C)

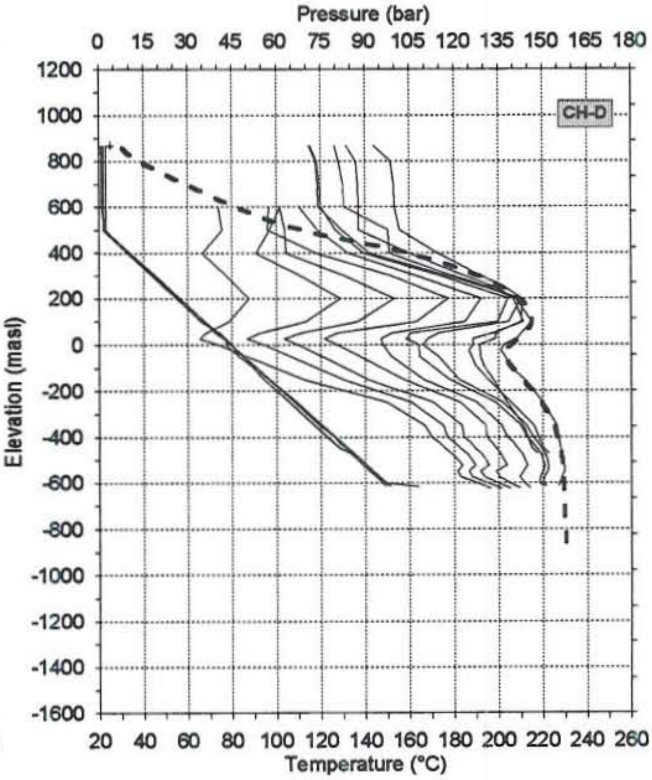
Pressure (bar)
0 15 30 45 60 75 90 105 120 135 150 165 180
CH-D
Elevation (masl)
1200 1000 800 600 400 200 0 -200 -400 -600 -800 -1000 -1200 -1400 -1600
20 40 60 80 100 120 140 160 180 200 220 240 260
Temperature (°C)

APPENDIX III: RELATIONS BETWEEN LUMPED MODEL AND RESERVOIR PROPERTIES

The storativity for the different types of reservoirs are:

- *Confined reservoir* $s = \rho_w[\phi c_w + (1 - \phi)c_r]$

- *Unconfined reservoir* $s = \phi / gH$

The conversion of resistances to reservoir permeability depends on the geometry of the conductor and one may assume either one dimensional (1-D) or two dimensional (2-D) fluid flow. For the 1-D case the fluid travels from one tank to another over a distance L from the centre of the first tank to the centre of the second tank through a common area A and common conductance σ_j (Figure 1).

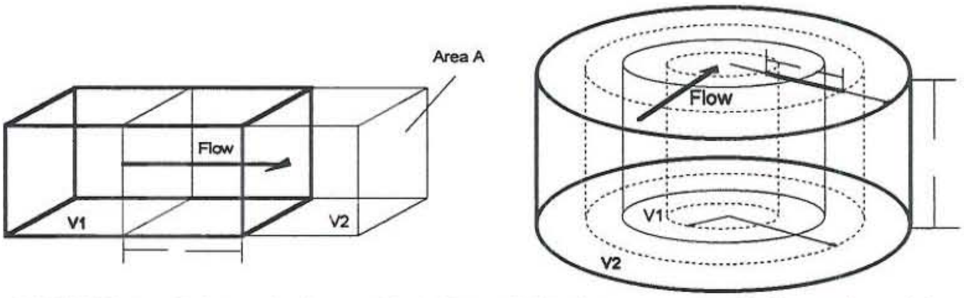

FIGURE 1: Schematic figures for 1-D and 2-D flow geometry in lumped models

The relation between permeability, k, and conductance, σ, for the 1-D case is given by the geometry and hydraulic parameters of the reservoir shown in the following equation, where μ is the kinematic fluid viscosity:

$$k = \sigma_i L \mu / A$$

This relation is connected to the volume of the tanks and consequently to the storage coefficients, κ_j, and conductance coefficients, σ_j, as follows, where A is the cross-section area of the flow and s is the storativity:

$$k = \frac{\sigma_j (\kappa_j + \kappa_{j+1}) \mu}{2A^2 s}$$

In the 2-D flow the fluid flows radially between two concentric tanks as is shown in Figure 1, from the middle section of the external tank, r_2, to the middle section of the internal tank, r_1, over a distance $L = r_2 - r_1$. In this case the relation between permeability, reservoir geometry, and conductance, σ, is the following:

$$k = \sigma_j \ln(\frac{r_{j+1}}{r_j}) \mu / (2 \pi h)$$

This equation can be connected to the volumes of the tank through the capacitance coefficients, κ_j, as follow:

$$k = [\sigma_j \ln(1 + \sqrt{1 + \frac{\kappa_{j+1}}{\kappa_j}})] / (2 \pi h)$$

where h is the thickness of the tanks.